Published for SISSA by Springer

Received: *July 3, 2024*
Accepted: *August 4, 2024*
Published: *August 29, 2024*

Azimuthal anisotropy of jet particles in p-Pb and Pb-Pb collisions at $\sqrt{s_{NN}} = 5.02$ TeV

The ALICE collaboration

E-mail: ALICE-publications@cern.ch

Abstract: The azimuthal anisotropy of particles associated with jets (jet particles) at midrapidity is measured for the first time in p-Pb and Pb-Pb collisions at $\sqrt{s_{NN}} = 5.02$ TeV down to transverse momentum (p_T) of 0.5 GeV/c and 2 GeV/c, respectively, with ALICE. The results obtained in p-Pb collisions are based on a novel three-particle correlation technique. The azimuthal anisotropy coefficient v_2 in high-multiplicity p-Pb collisions is positive, with a significance reaching 6.8σ at low p_T, and its magnitude is smaller than in semicentral Pb-Pb collisions. In contrast to the measurements in Pb-Pb collisions, the v_2 coefficient is also found independent of p_T within uncertainties. Comparisons with the inclusive charged-particle v_2 and with AMPT calculations are discussed. The predictions suggest that parton interactions play an important role in generating a non-zero jet-particle v_2 in p-Pb collisions, even though they overestimate the reported measurement. These observations shed new insights on the understanding of the origin of the collective behaviour of jet particles in small systems such as p-Pb collisions, and provide significant stringent new constraints to models.

Keywords: Heavy Ion Experiments, Jets, Particle Correlations and Fluctuations

ArXiv ePrint: 2212.12609

https://doi.org/10.1007/JHEP08(2024)234

Contents

1 Introduction

The study of ultrarelativistic heavy-ion collisions aims to investigate the properties of strongly-interacting matter characterised by high energy density and temperature, known as the quark-gluon plasma (QGP) [1, 2]. In non-central collisions, the initial spatial anisotropy of the overlap region of the colliding nuclei is converted into an anisotropy in momentum space via interactions among the medium constituents. The final-state anisotropies are quantified by the coefficients (v_n) of a Fourier decomposition of the azimuthal (φ) distribution of produced particles [3, 4]:

$$\frac{\mathrm{d}^2N}{\mathrm{d}p_\mathrm{T}\mathrm{d}\varphi} = \frac{1}{2\pi}\frac{\mathrm{d}N}{\mathrm{d}p_\mathrm{T}}\left(1 + 2\sum_{n=1}^{\infty} v_n(p_\mathrm{T})\cos[n(\varphi - \Psi_n)]\right), \tag{1.1}$$

where p_T is the transverse momentum and Ψ_n is the azimuthal angle of the symmetry plane for the n^{th} harmonic. Measurements of the v_n coefficients are expected to provide information on the initial state and the transport properties of the produced medium. The dominant coefficient is the second Fourier coefficient v_2, referred to as the elliptic flow [4, 5], which provides information on the collective expansion of the medium at low p_T [6] and the path-length dependence of medium-induced parton energy loss at high p_T [7, 8].

Collisions of small systems such as proton-nucleus are studied in detail to characterise the cold nuclear matter (CNM) effects which are also present in heavy-ion collisions, providing critical information for understanding QGP properties. These CNM effects influence parton distribution functions [9], induce Cronin-like effects [10], and cause energy loss [11]. As in heavy-ion collisions, a significant v_2 was observed in p-Pb collisions for soft as well as hard probes, such as open heavy-flavour hadrons [12, 13], quarkonia [14, 15], and high-p_T charged hadrons [16, 17]. A positive v_2 was also reported for charged particles [18–22] and muons from charm-hadron decays [23] in pp collisions, while the v_2 of muons from

JHEP08(2024)234

beauty-hadron decays was consistent with zero [23]. The observation of a non-zero v_2 in small collision systems raised the question whether small-size QGP droplets are formed in these conditions. However, the particle yields at high p_{T} in p-Pb collisions are found to be unmodified within uncertainties compared to the same measurements in pp collisions, scaled by the number of binary nucleon-nucleon collisions [17, 24–29]. Such an observation indicates that final-state effects are not significant in small collision systems. Therefore, alternative scenarios have been proposed, including color exchange in the final state [30], initial-state effects due to gluon saturation [31–33], or anisotropic escape of partons from the surface of the interaction zone [34].

This paper reports the first measurements of the p_{T}-differential v_2 of jet particles (particles associated with jets) at midrapidity in high-multiplicity p-Pb collisions and semicentral Pb-Pb collisions at $\sqrt{s_{\mathrm{NN}}} = 5.02\,\mathrm{TeV}$ with ALICE. The jet-particle v_2 measured down to lower p_{T} compared to the v_2 of reconstructed jets is of particular interest since it is clearly separated from particles from soft processes. These results are compared with inclusive charged-particle v_2 measurements in both p-Pb and Pb-Pb collisions, as well as with previous results of the v_2 of reconstructed jets in Pb-Pb collisions at $\sqrt{s_{\mathrm{NN}}} = 2.76\,\mathrm{TeV}$ [35]. Comparisons with A MultiPhase Transport (AMPT) model predictions [36, 37] are also discussed.

The article is organised as follows. Section 2 presents the ALICE apparatus with an emphasis on the detectors used in the analysis and the data taking conditions. The analysis strategy and the estimation of systematic uncertainties are described in section 3. Section 4 presents the results for jet particles and inclusive charged particles measured in p-Pb and Pb-Pb collisions as well as comparisons with AMPT model calculations in p-Pb collisions. Concluding remarks are drawn in section 5.

2 Experimental apparatus and data samples

The analysis is performed on the p-Pb and Pb-Pb data collected with the ALICE detector in 2016 and 2015, respectively. In p-Pb collisions, the asymmetry of the proton and Pb beam energies results in a rapidity shift of the nucleon-nucleon centre-of-mass by 0.465 in the direction of the proton beam with respect to the laboratory frame. In the following, the pseudorapidity η values correspond to the laboratory frame. A detailed description of the detector and its performance is given in refs. [38, 39]. The analysis is based on tracks reconstructed using the Time Projection Chamber (TPC) [40] located inside a large solenoidal magnet with a 0.5 T field parallel to the LHC beam direction and covering $|\eta| < 0.9$. Information from the Inner Tracking System (ITS) [41] is used to improve the spatial and momentum resolution of the reconstructed tracks. The Silicon Pixel Detector (SPD) [41, 42], comprising the two innermost layers of the ITS covering $|\eta| < 2.0$ and $|\eta| < 1.4$, is employed together with the TPC to determine the position of the primary interaction vertex. The Forward Multiplicity Detector (FMD) [43] consists of three sets of silicon strip sensors, covering $-3.5 < \eta < -1.7$ (FMD3) and $1.7 < \eta < 5$ (FMD1,2). The FMD is used in p-Pb collisions for the event selection and to extract the v_2 coefficient via long-range three-particle correlations. The V0 detector, formed by two scintillator arrays covering $-3.7 < \eta < -1.7$ (V0C) and $2.8 < \eta < 5.1$ (V0A), is used for triggering, event characterisation and centrality

JHEP08(2024)234

determination [44]. Two sets of Zero Degree Calorimeters (ZDC) [39], located at ± 112.5 m from the nominal interaction point along the beam line, are also used for the event selection.

The analysis of the p-Pb and Pb-Pb samples is based on events selected by a minimum bias (MB) trigger. The MB trigger is provided by the coincidence of signals in the two V0 scintillator arrays. Pile-up events are removed based on an event selection which uses the information from the V0 and SPD to tag events with multiple vertices. The beam-induced background is reduced offline by exploiting the V0 and ZDC timing information. In addition, in p-Pb collisions, the correlation between the multiplicity measured in the FMD and V0 is used to further remove contamination from beam-induced background and outliers in the FMD multiplicity distribution. Only events with a primary vertex along the beam axis, z_{vtx}, within ± 10 cm from the nominal interaction point are considered. About 526 million p-Pb and 60 million Pb-Pb events passed the event selection criteria. In Pb-Pb collisions, the centrality classes are defined as percentiles of the Pb-Pb hadronic cross section, and determined using the total energy deposited in the V0 arrays [45]. The p-Pb data sample is divided into several multiplicity classes based on the energy deposited in the V0A scintillators, located in the Pb-going direction [45]. In the p-Pb analysis, only the high-multiplicity class 0–10% and the low-multiplicity class 60–100% are studied. The measurements in Pb-Pb collisions are presented in the 20–60% centrality interval.

Reconstructed charged-particle tracks are selected by applying the standard conditions given in refs. [46–48]. They concern the number of space points and the quality of the track fit in the TPC, and the distance of closest approach to the primary vertex. Tracks are selected with $p_{\mathrm{T}} > 0.5\,\mathrm{GeV}/c$ and $|\eta| < 0.8$ in both p-Pb and Pb-Pb collisions. Hits in the FMD are measured in the η regions limited to $-3.2 < \eta < -1.8$ and $1.8 < \eta < 4.8$.

3 Data analysis

The procedure developed to calculate the jet-particle v_2 is detailed in ref. [48]. The jet-particle v_2 measurement consists of four main parts: (i) construction of the two-particle (charged particles at midrapidity regarded as trigger and associated particles) correlation function, (ii) extraction of the near-side jet peak (the signal) and background yields containing also the away-side jet yields, by fitting the two-particle correlation function, (iii) calculation of the v_2 of particle pairs represented by the trigger particles using three-particle correlations in p-Pb collisions, for the first time, and the scalar product method with the three-subevent technique in Pb-Pb collisions, and (iv) extraction of the v_2 of jet particles, in given trigger- and associated-particle p_{T} intervals, using a two-component fit function that takes into account the relative contribution from both jets and background to the particle-pair v_2.

3.1 Extraction of the near-side jet and background contributions

The two-dimensional correlation function is constructed as a function of the azimuthal angle difference ($\Delta\varphi$) and pseudorapidity difference ($\Delta\eta$) between trigger and associated particles (see refs. [14, 49] and references therein). Only pairs of particles with the same electric charge are considered to suppress correlations originating from resonance decays. The p_{T} of trigger particles ($p_{\mathrm{T}}^{\mathrm{trig}}$) is taken to be larger than that of associated particles ($p_{\mathrm{T}}^{\mathrm{assoc}}$) to avoid double counting of pairs. The correlation distribution is corrected for the limited two-particle

JHEP08(2024)234

acceptance and detector inhomogeneities by using the event-mixing technique [50], and normalized to the total number of trigger particles. Therefore, the correlation function is expressed in terms of the associated yield per trigger particle Y as

$$Y = \frac{1}{N_{\rm trig}} \frac{{\rm d}^2 N_{\rm assoc}}{{\rm d}\Delta\eta {\rm d}\Delta\varphi} = \frac{SE(\Delta\eta, \Delta\varphi)}{ME(\Delta\eta, \Delta\varphi)}, \tag{3.1}$$

where $N_{\rm trig}$ is the total number of trigger particles in a given event class. The signal distribution $SE(\Delta\eta, \Delta\varphi)$, given by $\frac{1}{N_{\rm trig}} \frac{{\rm d}^2 N_{\rm same}}{{\rm d}\Delta\eta {\rm d}\Delta\varphi}$, corresponds to the associated yield per trigger particle for particle pairs from the same event, and the background distribution $ME(\Delta\eta, \Delta\varphi) = \alpha \frac{{\rm d}^2 N_{\rm mix}}{{\rm d}\Delta\eta {\rm d}\Delta\varphi}$ is obtained by correlating trigger particles in an event with associated particles from other events of same event class. The α factor is introduced to normalise the background distribution to unity in the region of maximum pair acceptance. The same strategy is employed in Pb-Pb collisions.

Figure 1 (top-left) shows a typical example of the two-dimensional correlation distribution in high-multiplicity (0–10%) p-Pb collisions at $\sqrt{s_{\rm NN}} = 5.02\,{\rm TeV}$ for $3 < p_{\rm T}^{\rm trig} < 5\,{\rm GeV}/c$ and $1 < p_{\rm T}^{\rm assoc} < p_{\rm T}^{\rm trig}\,{\rm GeV}/c$. A near-side jet structure is clearly observed at $(\Delta\varphi \sim 0, \Delta\eta \sim 0)$ on top of the background. The distribution is fitted with a double Gaussian and a sum of Fourier harmonics up to the fifth order [51] (figure 1, top-right). The former is used to extract the near-side jet-peak yield (figure 1, bottom-left), and the latter serves to obtain the background yield (figure 1, bottow-right).

Similar typical distributions are also depicted in figure 2 for semicentral (20–60%) Pb-Pb collisions at $\sqrt{s_{\rm NN}} = 5.02\,{\rm TeV}$ for pairs of charged particles measured in $|\eta| < 0.8$ with $5 < p_{\rm T}^{\rm trig} < 6\,{\rm GeV}/c$ and $2 < p_{\rm T}^{\rm assoc} < p_{\rm T}^{\rm trig}\,{\rm GeV}/c$ in semicentral (20–60%) Pb-Pb collisions at $\sqrt{s_{\rm NN}} = 5.02\,{\rm TeV}$. A near-side jet structure is also clearly observed at $(\Delta\varphi \sim 0, \Delta\eta \sim 0)$ on top of the background which is as expected, more important than in p-Pb collisions.

3.2 Determination of the v_2 coefficient of particle pairs

In the p-Pb analysis, the v_2 of particle pairs, $v_2(\Delta\varphi, \Delta\eta)$, is computed by using long-range three-particle correlations. The trigger particles in particle pairs for a given ($\Delta\varphi$, $\Delta\eta$) cell are correlated with particles selected in $1.8 < \eta < 4.8$ using FMD1,2 to construct the long-range correlation distribution as a function of their azimuthal angle difference ($\Delta\varphi'$) and pseudorapidity difference ($\Delta\eta'$). Nonflow contributions, such as dijets, are suppressed by subtracting the scaled ($\Delta\varphi'$, $\Delta\eta'$) correlation functions measured in low-multiplicity (60–100%) collisions following the procedure described in refs. [19, 49, 52], where the scaling factor is the ratio of the away-side jet yield in high-multiplicity collisions to that in low-multiplicity collisions. For each $\Delta\varphi'$ interval, the $\Delta\eta'$ distribution in the $-5.6 < \Delta\eta' < -1.0$ range is integrated using a first-order polynomial fit to reduce the statistical fluctuations at the edges of $\Delta\eta'$ [52]. This $\Delta\varphi'$ distribution is fitted with a Fourier series parameterised with the first three harmonics as

$$\frac{{\rm d}N}{{\rm d}\Delta\varphi'} = a_0(\Delta\varphi, \Delta\eta) + 2\sum_{n=1}^{3} a_n(\Delta\varphi, \Delta\eta)\cos(n\Delta\varphi') \propto 1 + 2\sum_{n=1}^{3} V_{n\Delta}(\Delta\varphi, \Delta\eta)\cos(n\Delta\varphi'). \tag{3.2}$$

JHEP08(2024)234

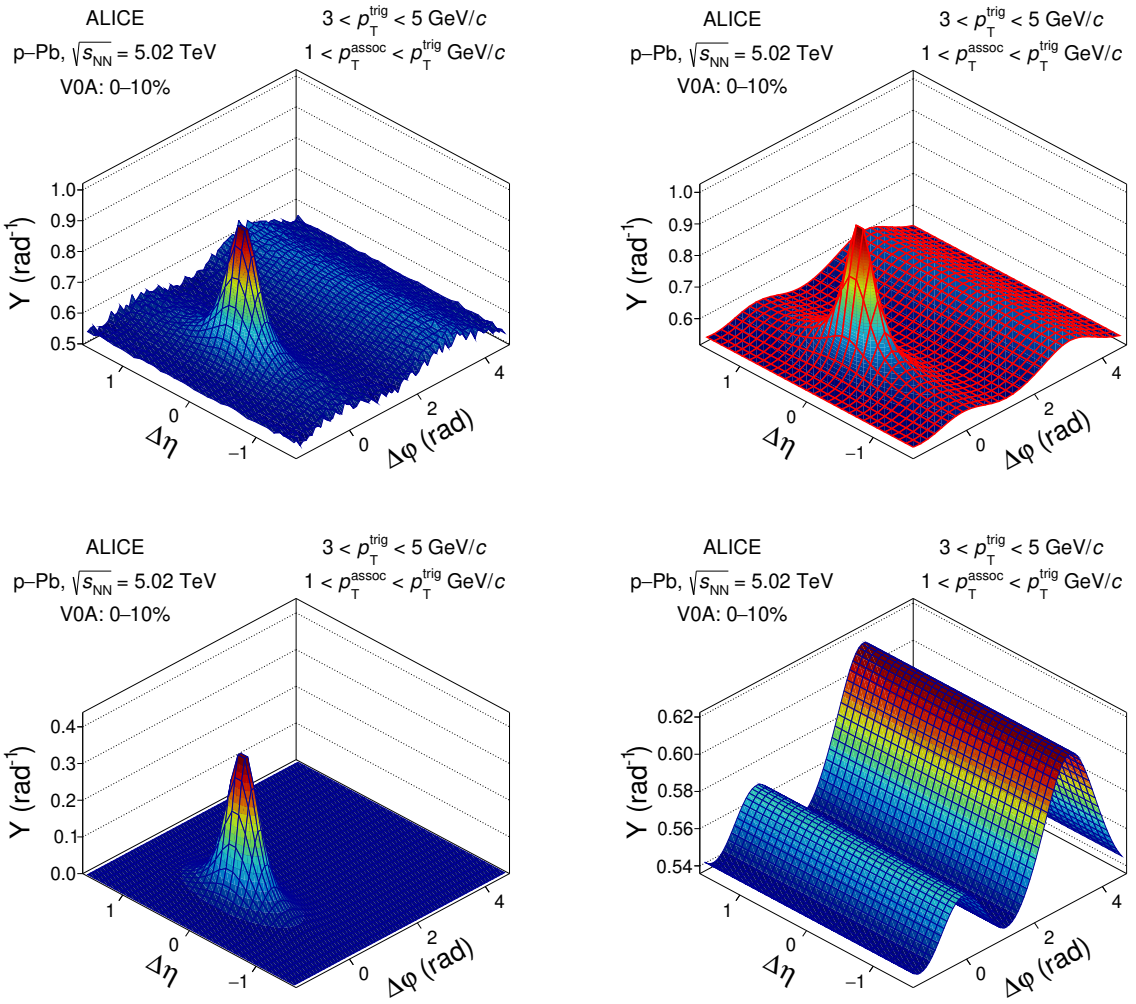

Figure 1. Top: raw associated yield per trigger particle Y (left) as a function of $\Delta\eta$ and $\Delta\varphi$ for pairs of charged particles measured in $|\eta| < 0.8$ with $3 < p_{\mathrm{T}}^{\mathrm{trig}} < 5\,\mathrm{GeV}/c$ and $1 < p_{\mathrm{T}}^{\mathrm{assoc}} < p_{\mathrm{T}}^{\mathrm{trig}}\,\mathrm{GeV}/c$ in high-multiplicity (0–10%) p-Pb collisions at $\sqrt{s_{\mathrm{NN}}} = 5.02\,\mathrm{TeV}$, and fit of the distribution (right). Bottom: extracted jet-particle (left) and background (right) yields.

The $V_{2\Delta}(\Delta\varphi, \Delta\eta)$ second-order Fourier coefficient is extracted from the fit parameters and is further expressed relative to the baseline. The latter is estimated from the integral in $\Delta\varphi'$ of the scaled correlation distribution in the low-multiplicity class around the minimum. The procedure is repeated for each p_{T} interval of trigger and associated charged particles. Figure 3 shows an example of the per-trigger associated yield as a function of $\Delta\eta'$ and $\Delta\varphi'$ for $3 < p_{\mathrm{T}}^{\mathrm{trig}} < 5\,\mathrm{GeV}/c$, $1 < p_{\mathrm{T}}^{\mathrm{assoc}} < p_{\mathrm{T}}^{\mathrm{trig}}\,\mathrm{GeV}/c$, $-0.9 < \Delta\eta < -0.7$ and $3.7 < \Delta\varphi < 4.2$ in high-multiplicity (top-left) and low-multiplicity (top-right) p-Pb collisions. The per-trigger associated yield in high-multiplicity p-Pb collisions after the subtraction of the scaled correlation distribution in the low-multiplicity class and the fit of the corresponding distribution with eq. (3.2) are displayed in the bottom-left and bottom-right panels, respectively.

Assuming that $V_{2\Delta}(\Delta\varphi, \Delta\eta)$ can be factorised as the product of single-particle v_2 coefficients, the v_2 of particle pairs represented by trigger particles ($v_2(\Delta\varphi, \Delta\eta)$) is expressed as the

JHEP08(2024)234

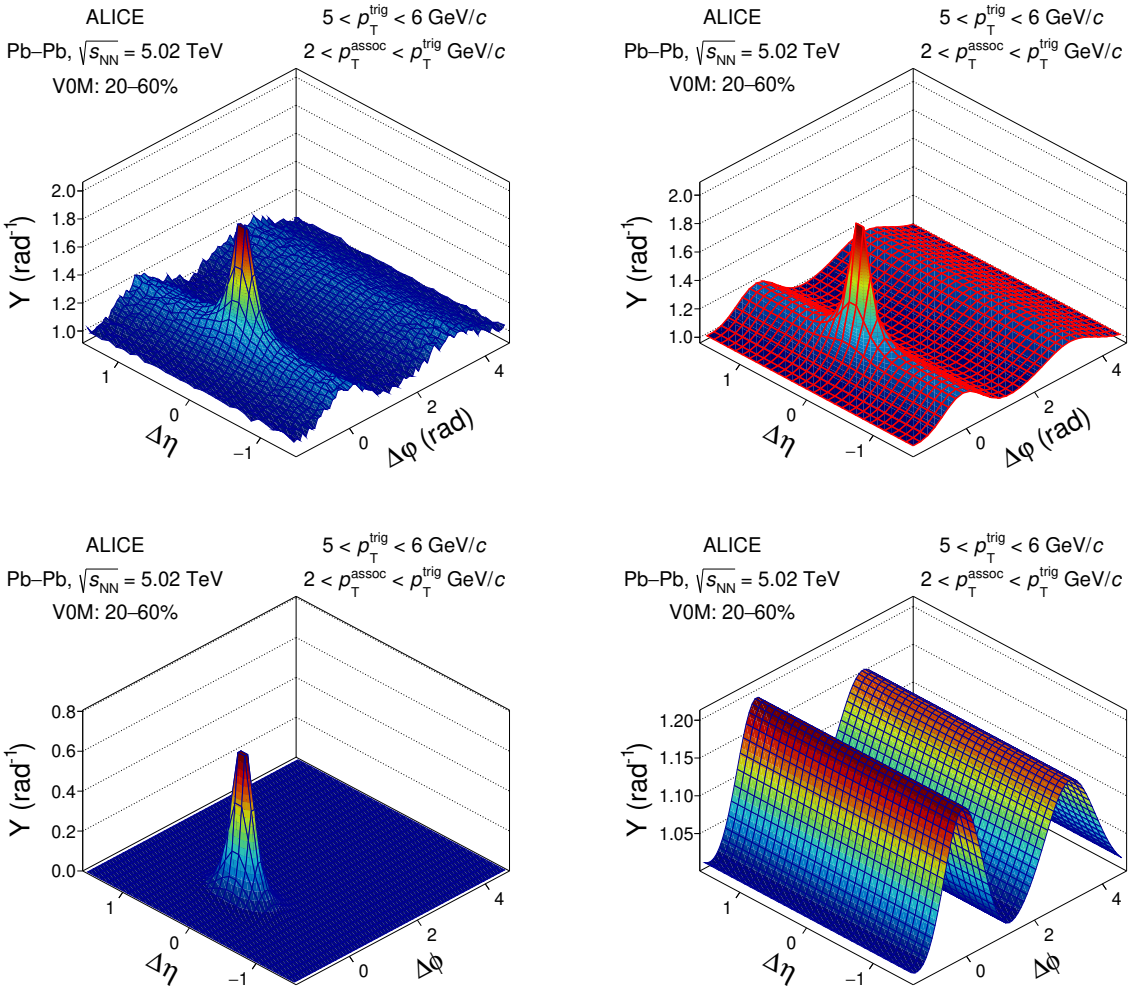

Figure 2. Top: raw associated yield per trigger particle Y (left) as a function of $\Delta\eta$ and $\Delta\varphi$ for pairs of charged particles measured in $|\eta| < 0.8$ with $5 < p_{\mathrm{T}}^{\mathrm{trig}} < 6\,\mathrm{GeV}/c$ and $2 < p_{\mathrm{T}}^{\mathrm{assoc}} < p_{\mathrm{T}}^{\mathrm{trig}}\,\mathrm{GeV}/c$ in high-multiplicity (0–10%) Pb-Pb collisions at $\sqrt{s_{\mathrm{NN}}} = 5.02\,\mathrm{TeV}$, and fit of the distribution (right). Bottom: extracted jet-particle (left) and background (right) yields.

ratio between the $V_{2\Delta}(\Delta\varphi, \Delta\eta)$ and the v_2 of particles in FMD1,2 ($v_2^{\mathrm{FMD1,2}}$). The $v_2^{\mathrm{FMD1,2}}$ is obtained with the three-subevent technique [53] by constructing long-range two-particle correlations between trigger and associated particles in TPC-FMD1,2, TPC-FMD3 and FMD1,2–FMD3 [54]. If the factorisation holds, the $v_2^{\mathrm{FMD1,2}}$ which is given by

$$v_2^{\mathrm{FMD1,2}} = \sqrt{\frac{V_{2\Delta}^{\mathrm{FMD1,2-FMD3}} V_{2\Delta}^{\mathrm{TPC-FMD1,2}}}{V_{2\Delta}^{\mathrm{TPC-FMD3}}}}, \tag{3.3}$$

amounts to 0.028 (with negligible uncertainties) in the 0–10% high-multiplicity class p-Pb collisions. The effect of the contamination of secondary particles is discussed in section 3.3.

In Pb-Pb collisions, the $v_2(\Delta\varphi, \Delta\eta)$ coefficient is extracted from the scalar product method via the three-subevent technique [55, 56]. The method correlates particle pairs measured in the TPC with the second-order event flow vector $\mathbf{Q}_2^{\mathrm{V0A}}$ estimated from the azimuthal distribution

JHEP08(2024)234

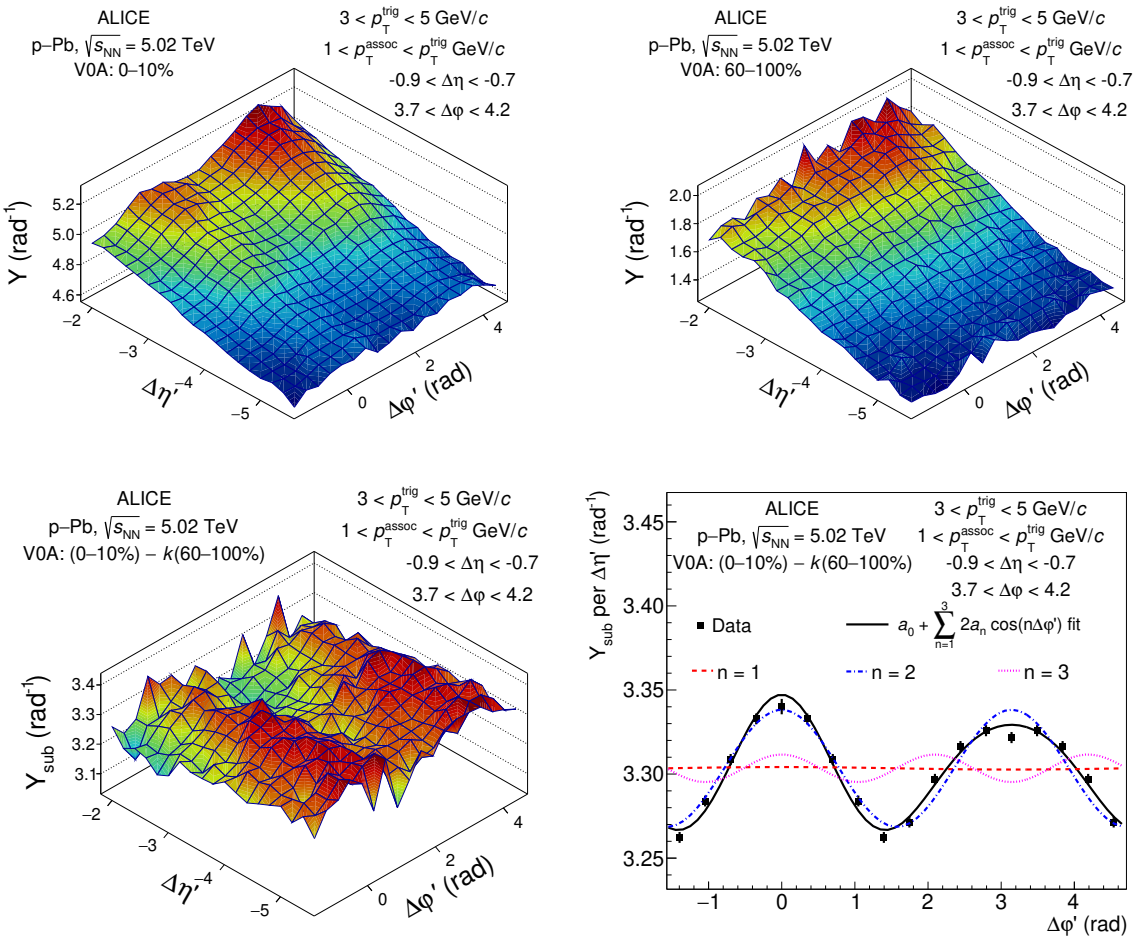

Figure 3. Top: example of the associated yield per-trigger particle Y in TPC-FMD1,2 correlations as a function of $\Delta\eta'$ and $\Delta\varphi'$ for $|\eta| < 0.8$ with $3 < p_{\mathrm{T}}^{\mathrm{trig}} < 5\,\mathrm{GeV}/c$, $1 < p_{\mathrm{T}}^{\mathrm{assoc}} < p_{\mathrm{T}}^{\mathrm{trig}}\,\mathrm{GeV}/c$, $-0.9 < \Delta\eta < -0.7$ and $3.7 < \Delta\varphi < 4.2$ in high-multiplicity (left) and low-multiplicity (right) p-Pb collisions at $\sqrt{s_{\mathrm{NN}}} = 5.02\,\mathrm{TeV}$. Bottom: associated per-trigger yield after the subtraction of the scaled correlation distribution in low-multiplicity collisions (left) and fit of the distribution projected onto $\Delta\varphi'$ with eq. (3.2).

of the energy deposited in the V0A. Therefore, the resulting $v_2(\Delta\varphi, \Delta\eta)$ is defined as

$$v_2(\Delta\varphi, \Delta\eta) = \langle \mathbf{u}_2(\Delta\varphi, \Delta\eta) \cdot \mathbf{Q}_2^{\mathrm{V0A}*} \rangle_{\mathrm{TPC-TPC}} \Big/ \sqrt{\frac{\langle \mathbf{Q}_2^{\mathrm{V0A}*} \cdot \mathbf{Q}_2^{\mathrm{V0C}} \rangle \langle \mathbf{Q}_2^{\mathrm{V0A}} \cdot \mathbf{Q}_2^{\mathrm{SPD}*} \rangle}{\langle \mathbf{Q}_2^{\mathrm{V0C}} \cdot \mathbf{Q}_2^{\mathrm{SPD}*} \rangle}}, \tag{3.4}$$

where $\mathbf{u}_2(\Delta\varphi, \Delta\eta)$ is the unit flow vector of each particle measured in the TPC. The second-order harmonic event flow vectors $\mathbf{Q}_2^{\mathrm{V0C}}$ and $\mathbf{Q}_2^{\mathrm{SPD}}$ measured in the V0C and SPD, respectively, are introduced to take into account the resolution of the event flow vector $\mathbf{Q}_2^{\mathrm{V0A}}$. The symbol * represents the complex conjugate and the bracket $\langle \dots \rangle_{\mathrm{TPC-TPC}}$ denotes the average over charged-particle pairs in a given p_{T} interval for trigger and associated particles, and centrality range. The brackets in the denominator denote the average over all events in a centrality class containing the particle pair. A recentering procedure is applied to correct the event flow

JHEP08(2024)234

vectors for the non-uniform azimuthal acceptance effects of the corresponding detectors [57]. The pseudorapidity gaps between the TPC and V0A, and the V0A, V0C, and SPD detectors suppress nonflow effects [47] and eliminate autocorrelations [58].

In both p-Pb and Pb-Pb collisions, the $v_2(\Delta\varphi, \Delta\eta)$ can be written [58, 59] as the weighted sum of the v_2 of jet particles ($v_2^{\text{jet part}}$) and background ($v_2^{\text{B}}(\Delta\varphi)$), as

$$v_2(\Delta\varphi, \Delta\eta) = \frac{S(\Delta\varphi, \Delta\eta)}{S(\Delta\varphi, \Delta\eta) + B(\Delta\varphi, \Delta\eta)} v_2^{\text{jet part}} + \frac{B(\Delta\varphi, \Delta\eta)}{S(\Delta\varphi, \Delta\eta) + B(\Delta\varphi, \Delta\eta)} v_2^{\text{B}}(\Delta\varphi), \tag{3.5}$$

where the jet-particle $S(\Delta\varphi, \Delta\eta)$ and background $B(\Delta\varphi, \Delta\eta)$ yields are extracted from the two-particle correlation functions constructed in the TPC. The $v_2^{\text{jet part}}$ coefficient is obtained by parametrising $v_2^{\text{B}}(\Delta\varphi)$ with a Fourier series up to the fifth order and fitting eq. (3.5) to the measured $v_2(\Delta\varphi, \Delta\eta)$ distributions in a given p_{T} interval for trigger and associated particles.

An example of the measured $v_2(\Delta\varphi, \Delta\eta)$ distribution of particle pairs measured in p-Pb collisions at $\sqrt{s_{\text{NN}}} = 5.02\,\text{TeV}$ for $3 < p_{\text{T}}^{\text{trig}} < 5\,\text{GeV}/c$ and $1 < p_{\text{T}}^{\text{assoc}} < p_{\text{T}}^{\text{trig}}\,\text{GeV}/c$ is depicted in figure 4 (top-left), where a different structure is clearly seen in the region around the near-side jet peak ($\Delta\varphi \sim 0$, $\Delta\eta \sim 0$) compared to the background-dominated region. This is a first indication of a different behaviour for v_2 of jet and background particles. A similar structure is also visible in Pb-Pb collisions at $\sqrt{s_{\text{NN}}} = 5.02\,\text{TeV}$ for $5 < p_{\text{T}}^{\text{trig}} < 6\,\text{GeV}/c$ and $2 < p_{\text{T}}^{\text{assoc}} < p_{\text{T}}^{\text{trig}}\,\text{GeV}/c$ (figure 4, bottom-left). The corresponding fits with eq. (3.5) are shown in figure 4 (right panels).

For comparison, the v_2 coefficient of inclusive charged particles, v_2^{ch} is also computed. In p-Pb collisions, it is evaluated using the three-subevent technique by constructing long-range two-particle correlations, as done for the $v_2^{\text{FMD1,2}}$ calculation, and is expressed as

$$v_2^{\text{ch}} = \sqrt{\frac{V_{2\Delta}^{\text{TPC-FMD1,2}} V_{2\Delta}^{\text{TPC-FMD3}}}{V_{2\Delta}^{\text{FMD1,2-FMD3}}}}. \tag{3.6}$$

In Pb-Pb collisions, the v_2^{ch} is determined using the scalar product method with the three-subevent technique (see eq. (3.4)).

3.3 Estimation of systematic uncertainties

Details of the separate contributions to the systematic uncertainties are given in ref. [48]. The values for both jet particles in a representative $p_{\text{T}}^{\text{assoc}}$ interval and inclusive charged particles in p-Pb and Pb-Pb collisions are summarised in tables 1 and 2, respectively.

The jet-particle and inclusive charged-particle v_2 measurements in p-Pb collisions are affected by the following systematic uncertainties. The variation of the range of z_{vtx} and a less stringent condition on the correlation between the multiplicity estimates obtained with the FMD and V0, give the systematic uncertainties related to the event selection. The uncertainty on the track reconstruction is estimated by modifying the track selection criteria. The bias due to the contribution of secondary particles produced in the FMD acceptance on the jet-particle v_2 is investigated in AMPT simulations [36, 37, 60]. In order to check for residual nonflow effects after the subtraction of the scaled low-multiplicity event class,

JHEP08(2024)234

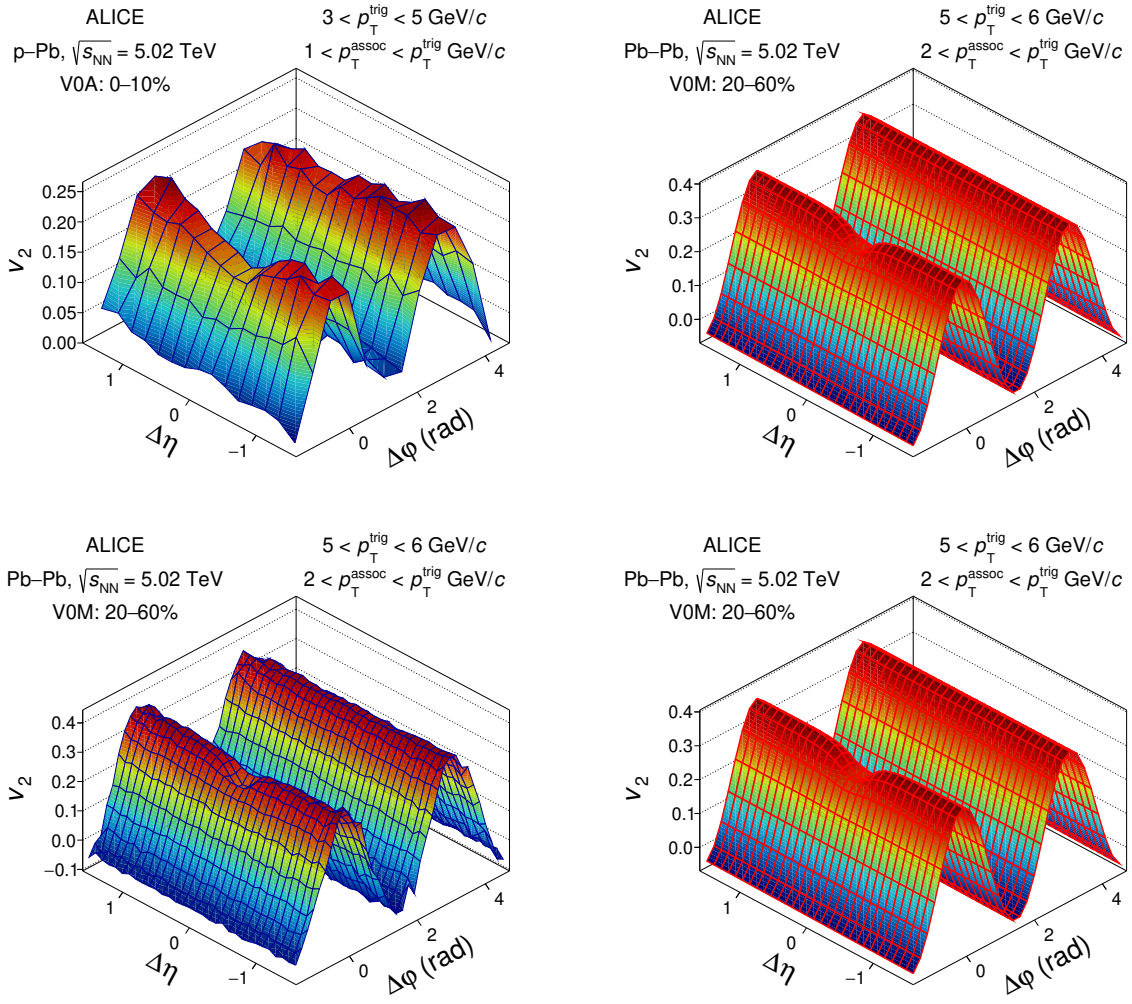

Figure 4. Left: $v_2(\Delta\varphi, \Delta\eta)$ distributions of charged particles measured at midrapidity in high-multiplicity (0–10%) p-Pb collisions at $\sqrt{s_{\rm NN}} = 5.02\,\text{TeV}$ (top) and semicentral (20–60%) Pb-Pb collisions at $\sqrt{s_{\rm NN}} = 5.02\,\text{TeV}$ (bottom). Right: fits fo the two corresponding distributions in p-Pb (top) and Pb-Pb (bottom) collisions. The $p_{\rm T}^{\rm trig}$ and $p_{\rm T}^{\rm assoc}$ intervals are mentioned in the legend.

the template fitting procedure [19] is tested. The difference between the two procedures is considered as a systematic uncertainty. A potential bias resulting from weak long-range correlations present in 60–100% low-multiplicity events is studied by changing the interval from 60–100% to 70–100%. A systematic effect arises from the procedure employed for the $\Delta\varphi'$. The $\Delta\varphi'$ projection in eq. (3.2) is obtained from a constant fit instead of using a first-order polynomial fit along each $\Delta\eta'$ interval. Finally, the baseline is also calculated in high-multiplicity collisions from the integral or from a second-order polynomial fit around the minimum at $\Delta\varphi' \sim \pi/2$. The last two sources are the systematic uncertainty on the v_2 calculation. The aforementioned sources are added in quadrature in each $p_{\rm T}$ interval of trigger and associated particles to obtain a total systematic uncertainty on the jet-particle v_2 in the range 11.2–34.3%. The total systematic uncertainty on the inclusive charged-particle which depends on the trigger-particle $p_{\rm T}$, is 4.4–25.3%.

JHEP08(2024)234

Source	Jet particles $p_{\mathrm{T}}^{\mathrm{assoc}} > 0.5\,\mathrm{GeV}/c$	Charged particles
Vertex selection	0.6–14.6%	0.02–1.30%
FMD-V0 correlation	0.1–7.9%	0.1–0.2%
Track selection	0.3–3.6%	0.0–2.2%
Secondaries in FMD	4%	4%
Residual nonflow	0.1–5.4%	0.1–13.2%
Remaining ridge	6.5–29.0%	0.7–20.7%
v_2 calculation	4.5–11.7%	0.7–1.5%
Total	11.2–34.3%	4.4–25.3%

Table 1. Systematic uncertainties on the jet-particle v_2 for $p_{\mathrm{T}}^{\mathrm{assoc}} > 0.5\,\mathrm{GeV}/c$ and the inclusive charged-particle v_2 in high-multiplicity (0–10%) p-Pb collisions at $\sqrt{s_{\mathrm{NN}}} = 5.02\,\mathrm{TeV}$. The systematic uncertainties vary within the indicated intervals depending on the p_{T} of trigger particles.

Source	Jet particles $p_{\mathrm{T}}^{\mathrm{assoc}} > 2\,\mathrm{GeV}/c$	Charged particles
Vertex selection	0.6–5.3%	0–5.3%
Pile-up	0.01–3.60%	0–2.7%
Centrality	0.3–1.4%	0–1.8%
Flow vector	0.3–1.4%	0–4.2%
Track selection	0.8–4.5%	0.01–1.80%
Total	1.6–7.3%	0.02–7.30%

Table 2. Systematic uncertainties on the jet-particle v_2 for $p_{\mathrm{T}}^{\mathrm{assoc}} > 2.0\,\mathrm{GeV}/c$ and the inclusive charged-particle v_2 in semicentral (20–60%) Pb-Pb collisions at $\sqrt{s_{\mathrm{NN}}} = 5.02\,\mathrm{TeV}$. The systematic uncertainties vary within the indicated intervals depending on the p_{T} of trigger particles.

In Pb-Pb collisions, in addition to the systematic uncertainties arising from the variation of the z_{vtx} range and track selection criteria listed for p-Pb collisions, a systematic uncertainty related to the centrality determination is estimated by using different centrality estimators. The systematic effect related to the pile-up event rejection is assessed via a dedicated analysis where pile-up events are not removed, only to estimate their importance. The event flow vector is computed by using V0C instead of V0A. All the systematic uncertainties are added in quadrature to obtain the total systematic uncertainty ranging from 1.6–10.1% and 0.02–7.30% for the jet-particle v_2 and inclusive charged-particle v_2, respectively.

4 Results and model comparisons

Figure 5 presents the v_2 of jet particles as a function of p_{T} at midrapidity ($|\eta| < 0.8$) for different $p_{\mathrm{T}}^{\mathrm{assoc}}$ intervals, in high-multiplicity (0–10%) p-Pb collisions at $\sqrt{s_{\mathrm{NN}}} = 5.02\,\mathrm{TeV}$. The

JHEP08(2024)234

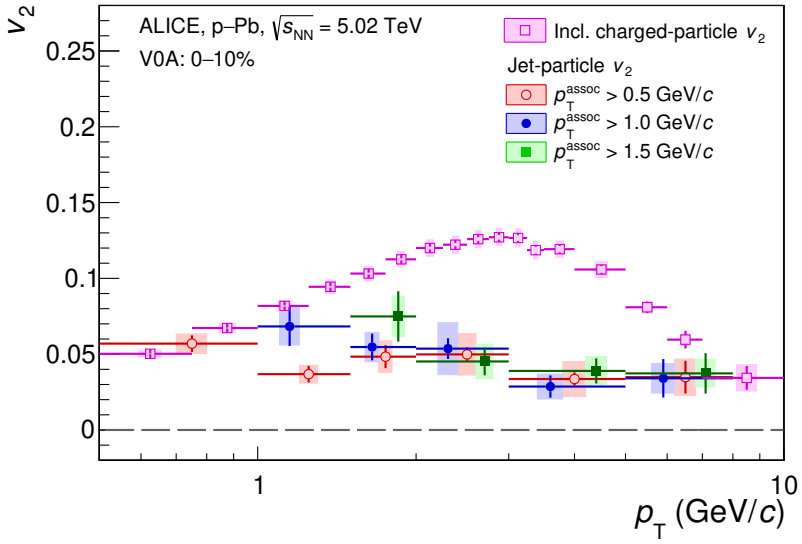

Figure 5. Jet-particle v_2 as a function of the trigger-particle p_T for several p_T^{assoc} intervals in 0–10% p-Pb collisions at $\sqrt{s_{NN}} = 5.02$ TeV, compared with the inclusive charged-particle v_2. The values of the jet-particle v_2 are horizontally shifted around the centre of the bin for better visibility. The statistical uncertainties, shown as vertical bars, are determined using the sub-sample technique. The systematic uncertainties are represented as filled boxes. Horizontal bars indicate the bin width.

p_T-differential inclusive charged-particle v_2 coefficient is also displayed. A positive jet-particle v_2 of ~ 0.04 is measured and it is independent of the p_T of trigger and associated particles within uncertainties. The significance is 2.6–6.8σ for $p_T \lesssim 5$ GeV/c, depending on both the p_T of trigger and associated particles. In contrast, the v_2 of inclusive charged particles which mostly originates from the underlying event, is larger in magnitude and presents a clear dependence on p_T. This constitutes the first experimental evidence of different mechanisms in play for the v_2 of soft and hard probes at low p_T in p-Pb collisions.

The jet-particle v_2 and the inclusive charged-particle v_2 are also measured in semicentral (20–60%) Pb-Pb collisions at $\sqrt{s_{NN}} = 5.02$ TeV, as shown in figure 6. The published v_2 of reconstructed jets measured in 30–50% Pb-Pb collisions at $\sqrt{s_{NN}} = 2.76$ TeV [35] is also displayed, extending the presented measurements up to $p_T = 90$ GeV/c. A positive jet-particle v_2 is measured for the first time in the low p_T region, down to $p_T = 2$ GeV/c. The jet-particle v_2 does not exhibit any dependence on the associated p_T, while it decreases with increasing p_T from $p_T \sim 3$ GeV/c, and converges towards the v_2 of inclusive charged particles for $p_T \gtrsim 7$ GeV/c. In the high p_T region ($p_T \gtrsim 10$ GeV/c), the uniform behaviour of the inclusive charged-particle v_2 and jet v_2 as a function of p_T is attributed to the path-length dependent parton energy loss in Pb-Pb collisions [46]. It can be noted that in this region, the jet-particle v_2 is consistent with the reconstructed jet v_2. In the interval $2 < p_T \lesssim 6$ GeV/c, the clear p_T dependence of the jet-particle v_2 in Pb-Pb collisions may be attributed to the interplay between hard partons and bulk particles.

The comparison of the v_2 results obtained in p-Pb (0–10%) and Pb-Pb (20–60%) collisions for jet particles and inclusive charged particles is discussed in figure 7. Since no significant dependence on p_T^{assoc} is evidenced for jet particles (see figures 5 and 6), the results are shown for

JHEP08(2024)234

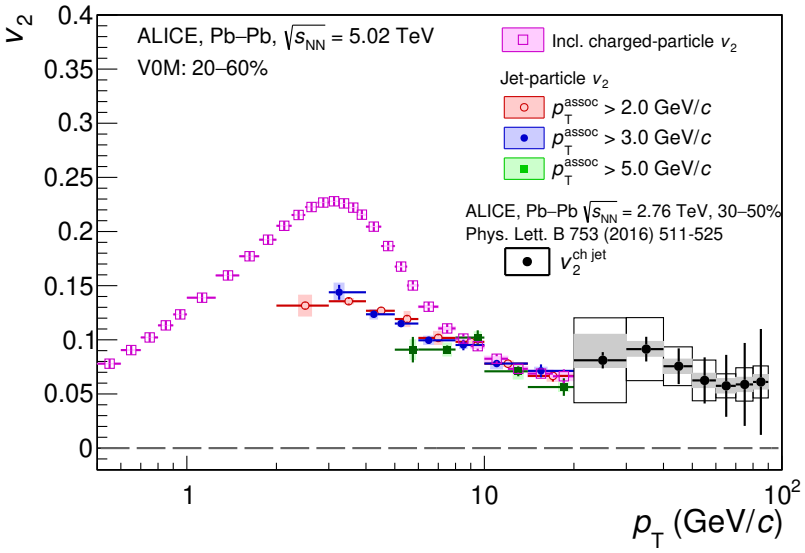

Figure 6. Jet-particle v_2 as a function of the trigger-particle p_{T} for several $p_{\mathrm{T}}^{\mathrm{assoc}}$ intervals in 20–60% Pb-Pb collisions at $\sqrt{s_{\mathrm{NN}}} = 5.02\,\mathrm{TeV}$, compared with the inclusive charged-particle v_2. The values of the jet-particle v_2 are horizontally shifted around the centre of the bin for better visibility. The statistical uncertainties, shown as vertical bars, are determined using the sub-sample technique. The systematic uncertainties are represented as filled boxes. Horizontal bars indicate the bin width. The published v_2 of reconstructed jets measured in 30–50% Pb-Pb collisions is also shown [35].

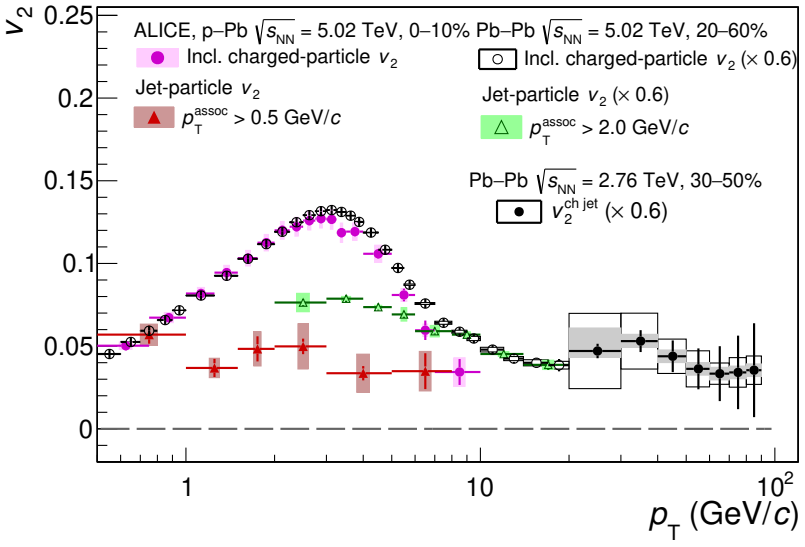

Figure 7. Comparison of the p_{T}-differential jet-particle and inclusive charged-particle v_2 measured in high-multiplicity p-Pb collisions at $\sqrt{s_{\mathrm{NN}}} = 5.02\,\mathrm{TeV}$ with the same measurements performed in semicentral Pb-Pb collisions. The published ALICE v_2 of reconstructed jets measured in 30–50% Pb-Pb collisions is also shown [35]. The results obtained in Pb-Pb collisions are scaled by a factor 0.6. See the text for the details.

JHEP08(2024)234

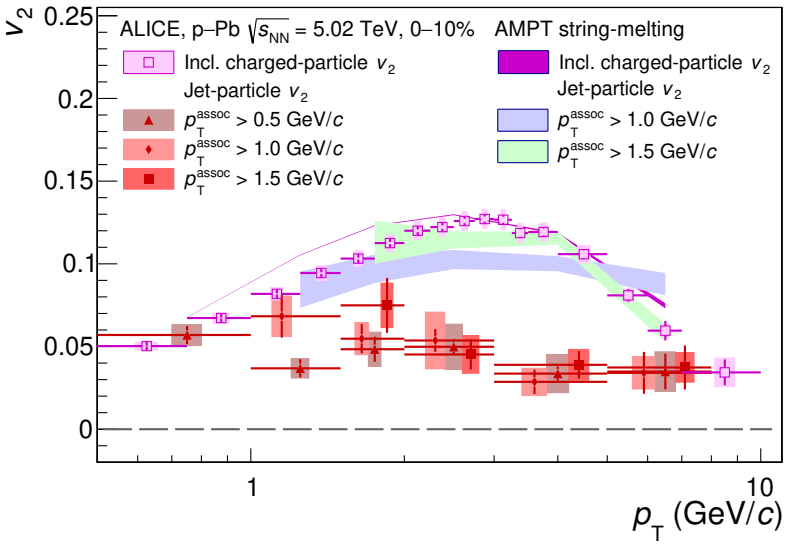

Figure 8. Comparison of the p_{T}-differential jet-particle and inclusive charged-particle v_2 measured in high-multiplicity p-Pb collisions at $\sqrt{s_{\mathrm{NN}}} = 5.02\,\mathrm{TeV}$ with AMPT calculations [36, 37].

the $p_{\mathrm{T}}^{\mathrm{assoc}}$ interval which allows us to cover the largest p_{T} range. The centrality class is chosen such that the eccentricity, which quantifies the initial spatial anisotropies, is close to that in high-multiplicity p-Pb collisions according to Glauber Monte Carlo simulations [61], although the charged-particle multiplicities reached in the heavier system are larger. The published v_2 of reconstructed jets measured in 30–50% Pb-Pb collisions at $\sqrt{s_{\mathrm{NN}}} = 2.76\,\mathrm{TeV}$ [35] are also included in the figure. A scaling factor of 0.6 is applied to the v_2 of inclusive charged particles, jet particles and reconstructed jets in Pb-Pb collisions to ensure that the low p_{T} ($p_{\mathrm{T}} \lesssim 3\,\mathrm{GeV}/c$) inclusive charged-particle v_2 matches that in p-Pb collisions. This factor may account for the slightly different spatial anisotropies in the two colliding systems and the larger multiplicity in the heaviest system [17]. After such scaling, the inclusive charged-particle v_2 in p-Pb collisions is compatible with that measured in Pb-Pb collisions. A different behaviour is evidenced for jet particles. In contrast to what is observed in Pb-Pb collisions, the jet-particle v_2 measured in p-Pb collisions is found independent of p_{T}. This suggests that the collectivity from the initial state survives throughout all stages in the system evolution more easily in p-Pb than Pb-Pb collisions [62]. This is also confirmed from the positive jet-particle v_2 measurement in p-Pb collisions without any indication of a modification of the jet production yields within experimental uncertainties [17, 25, 26].

Figure 8 presents a comparison of the jet-particle and inclusive charged-particle v_2 with the string-melting version of AMPT model (v2.26t9b) [36, 37, 60] in order to shed more light on the origin of the jet-particle v_2 measured in high-multiplicity p-Pb collisions. The AMPT model includes four main processes: (i) initial conditions obtained from the HIJING model [63, 64], (ii) parton scatterings based on the Zhang's parton cascade (ZPC) model [65], (iii) hadronisation via coalescence and (iv) hadronic interactions described by a relativistic transport (ART) model [66]. A parton scattering cross section of 3 mb is used [67]. Its value is obtained by adjusting the Debye screening mass so that the model describes the p_{T} distribution and the v_2 coefficient of identified particles measured in p-Pb collisions at $\sqrt{s_{\mathrm{NN}}}$

JHEP08(2024)234

= 5.02 TeV by the ALICE collaboration [68]. In this model, the v_2 is calculated following the same analysis procedure as with data and the event characterisation is done by mimicking the event class selection using the V0A detector at particle level, i.e. by counting charged particles in $2.8 < \eta < 5.1$. The AMPT calculations lead to a positive inclusive charged-particle and jet-particle v_2, indicating that parton interactions play an important role in the v_2 generation. The model provides a fair agreement with the measured inclusive charged-particle v_2, while it overestimates the measured jet-particle v_2, predicting a v_2 whose shape and magnitude are compatible with those of inclusive charged particles. This is possibly due to the fact that AMPT treats soft and hard components equally in the parton interaction stage, while the measurement indicates that hard partons interact with the underlying event differently from the bulk constituents themselves.

5 Summary

In summary, the jet-particle v_2 measured in high-multiplicity (0–10%) p-Pb collisions at $\sqrt{s_{\rm NN}} = 5.02$ TeV is assessed for the first time in the $p_{\rm T}$ range 0.5–8.0 GeV/c by means of a novel multi-particle correlation technique. The jet-particle v_2 is also measured down to low $p_{\rm T}$ in semicentral Pb-Pb collisions at $\sqrt{s_{\rm NN}} = 5.02$ TeV and is complementary to the previous jet v_2 results at higher $p_{\rm T}$. Comparisons with the inclusive charged-particle v_2 measured in both p-Pb and Pb-Pb collisions are discussed. A positive and $p_{\rm T}$-independent v_2 signal is observed with a significance reaching 6.8σ at low $p_{\rm T}$ in p-Pb collisions. The v_2 magnitude is smaller than that measured in Pb-Pb collisions at intermediate $p_{\rm T}$. In addition, a clear $p_{\rm T}$ dependence of the v_2 signal of jet particles is observed in Pb-Pb collisions. The comparison with AMPT predictions shows that parton interactions can generate a positive v_2 for jet particles in high-multiplicity p-Pb collisions. These new results bring crucial information about the origin of the observed azimuthal anisotropies of jet particles in p-Pb collisions and set key constraints on theoretical calculations.

Acknowledgments

The ALICE collaboration would like to thank all its engineers and technicians for their invaluable contributions to the construction of the experiment and the CERN accelerator teams for the outstanding performance of the LHC complex. The ALICE collaboration gratefully acknowledges the resources and support provided by all Grid centres and the Worldwide LHC Computing Grid (WLCG) collaboration. The ALICE collaboration acknowledges the following funding agencies for their support in building and running the ALICE detector: A.I. Alikhanyan National Science Laboratory (Yerevan Physics Institute) Foundation (ANSL), State Committee of Science and World Federation of Scientists (WFS), Armenia; Austrian Academy of Sciences, Austrian Science Fund (FWF): [M 2467-N36] and Nationalstiftung für Forschung, Technologie und Entwicklung, Austria; Ministry of Communications and High Technologies, National Nuclear Research Center, Azerbaijan; Conselho Nacional de Desenvolvimento Científico e Tecnológico (CNPq), Financiadora de Estudos e Projetos (Finep), Fundação de Amparo à Pesquisa do Estado de São Paulo (FAPESP) and Universidade Federal do Rio Grande do Sul (UFRGS), Brazil; Bulgarian Ministry of Education and Science, within the National Roadmap for Research Infrastructures 2020–2027 (object CERN), Bulgaria;

JHEP08(2024)234

Ministry of Education of China (MOEC), Ministry of Science & Technology of China (MSTC) and National Natural Science Foundation of China (NSFC), China; Ministry of Science and Education and Croatian Science Foundation, Croatia; Centro de Aplicaciones Tecnológicas y Desarrollo Nuclear (CEADEN), Cubaenergía, Cuba; Ministry of Education, Youth and Sports of the Czech Republic, Czech Republic; The Danish Council for Independent Research | Natural Sciences, the VILLUM FONDEN and Danish National Research Foundation (DNRF), Denmark; Helsinki Institute of Physics (HIP), Finland; Commissariat à l'Energie Atomique (CEA) and Institut National de Physique Nucléaire et de Physique des Particules (IN2P3) and Centre National de la Recherche Scientifique (CNRS), France; Bundesministerium für Bildung und Forschung (BMBF) and GSI Helmholtzzentrum für Schwerionenforschung GmbH, Germany; General Secretariat for Research and Technology, Ministry of Education, Research and Religions, Greece; National Research, Development and Innovation Office, Hungary; Department of Atomic Energy Government of India (DAE), Department of Science and Technology, Government of India (DST), University Grants Commission, Government of India (UGC) and Council of Scientific and Industrial Research (CSIR), India; National Research and Innovation Agency — BRIN, Indonesia; Istituto Nazionale di Fisica Nucleare (INFN), Italy; Japanese Ministry of Education, Culture, Sports, Science and Technology (MEXT) and Japan Society for the Promotion of Science (JSPS) KAKENHI, Japan; Consejo Nacional de Ciencia (CONACYT) y Tecnología, through Fondo de Cooperación Internacional en Ciencia y Tecnología (FONCICYT) and Dirección General de Asuntos del Personal Academico (DGAPA), Mexico; Nederlandse Organisatie voor Wetenschappelijk Onderzoek (NWO), The Netherlands; The Research Council of Norway, Norway; Commission on Science and Technology for Sustainable Development in the South (COMSATS), Pakistan; Pontificia Universidad Católica del Perú, Peru; Ministry of Education and Science, National Science Centre and WUT ID-UB, Poland; Korea Institute of Science and Technology Information and National Research Foundation of Korea (NRF), Republic of Korea; Ministry of Education and Scientific Research, Institute of Atomic Physics, Ministry of Research and Innovation and Institute of Atomic Physics and Universitatea Nationala de Stiinta si Tehnologie Politehnica Bucuresti, Romania; Ministry of Education, Science, Research and Sport of the Slovak Republic, Slovakia; National Research Foundation of South Africa, South Africa; Swedish Research Council (VR) and Knut & Alice Wallenberg Foundation (KAW), Sweden; European Organization for Nuclear Research, Switzerland; Suranaree University of Technology (SUT), National Science and Technology Development Agency (NSTDA) and National Science, Research and Innovation Fund (NSRF via PMU-B B05F650021), Thailand; Turkish Energy, Nuclear and Mineral Research Agency (TENMAK), Turkey; National Academy of Sciences of Ukraine, Ukraine; Science and Technology Facilities Council (STFC), United Kingdom; National Science Foundation of the United States of America (NSF) and United States Department of Energy, Office of Nuclear Physics (DOE NP), United States of America. In addition, individual groups or members have received support from: European Research Council, Strong 2020 — Horizon 2020, Marie Skłodowska Curie (grant nos. 950692, 824093, 896850), European Union; ICSC — Centro Nazionale di Ricerca in High Performance Computing, Big Data and Quantum Computing, European Union — NextGenerationEU; Academy of Finland (Center of Excellence in Quark Matter) (grant nos. 346327, 346328), Finland; Programa de Apoyos para la Superación del Personal Académico, UNAM, Mexico.

JHEP08(2024)234

References

[1] HotQCD collaboration, *Equation of state in* $(2+1)$*-flavor QCD*, *Phys. Rev. D* **90** (2014) 094503 [arXiv:1407.6387] [INSPIRE].

[2] E. Shuryak, *Strongly coupled quark-gluon plasma in heavy ion collisions*, *Rev. Mod. Phys.* **89** (2017) 035001 [arXiv:1412.8393] [INSPIRE].

[3] S.A. Voloshin and Y. Zhang, *Flow study in relativistic nuclear collisions by Fourier expansion of Azimuthal particle distributions*, *Z. Phys. C* **70** (1996) 665 [hep-ph/9407282] [INSPIRE].

[4] A.M. Poskanzer and S.A. Voloshin, *Methods for analyzing anisotropic flow in relativistic nuclear collisions*, *Phys. Rev. C* **58** (1998) 1671 [nucl-ex/9805001] [INSPIRE].

[5] J.-Y. Ollitrault, *Anisotropy as a signature of transverse collective flow*, *Phys. Rev. D* **46** (1992) 229 [INSPIRE].

[6] P.F. Kolb and U.W. Heinz, *Hydrodynamic description of ultrarelativistic heavy ion collisions*, SUNY-NTG-03-06 (2003) [nucl-th/0305084] [INSPIRE].

[7] M. Gyulassy, I. Vitev and X.-N. Wang, *High* p_T *azimuthal asymmetry in noncentral* $A+A$ *at RHIC*, *Phys. Rev. Lett.* **86** (2001) 2537 [nucl-th/0012092] [INSPIRE].

[8] E.V. Shuryaks, *The Azimuthal asymmetry at large* p_t *seem to be too large for a 'jet quenching'*, *Phys. Rev. C* **66** (2002) 027902 [nucl-th/0112042] [INSPIRE].

[9] K.J. Eskola, H. Paukkunen and C.A. Salgado, *EPS09: A New Generation of NLO and LO Nuclear Parton Distribution Functions*, *JHEP* **04** (2009) 065 [arXiv:0902.4154] [INSPIRE].

[10] B.Z. Kopeliovich, J. Nemchik, A. Schafer and A.V. Tarasov, *Cronin effect in hadron production off nuclei*, *Phys. Rev. Lett.* **88** (2002) 232303 [hep-ph/0201010] [INSPIRE].

[11] Z.-B. Kang, I. Vitev, E. Wang, H. Xing and C. Zhang, *Multiple scattering effects on heavy meson production in* $p+A$ *collisions at backward rapidity*, *Phys. Lett. B* **740** (2015) 23 [arXiv:1409.2494] [INSPIRE].

[12] ALICE collaboration, *Azimuthal Anisotropy of Heavy-Flavor Decay Electrons in p-Pb Collisions at* $\sqrt{s_{\rm NN}} = 5.02$ *TeV*, *Phys. Rev. Lett.* **122** (2019) 072301 [arXiv:1805.04367] [INSPIRE].

[13] CMS collaboration, *Studies of charm and beauty hadron long-range correlations in pp and pPb collisions at LHC energies*, *Phys. Lett. B* **813** (2021) 136036 [arXiv:2009.07065] [INSPIRE].

[14] ALICE collaboration, *Search for collectivity with azimuthal* J/ψ*-hadron correlations in high multiplicity p-Pb collisions at* $\sqrt{s_{\rm NN}} = 5.02$ *and* 8.16 *TeV*, *Phys. Lett. B* **780** (2018) 7 [arXiv:1709.06807] [INSPIRE].

[15] CMS collaboration, *Observation of prompt* J/ψ *meson elliptic flow in high-multiplicity pPb collisions at* $\sqrt{s_{\rm NN}} = 8.16$ *TeV*, *Phys. Lett. B* **791** (2019) 172 [arXiv:1810.01473] [INSPIRE].

[16] CMS collaboration, *Pseudorapidity and transverse momentum dependence of flow harmonics in pPb and PbPb collisions*, *Phys. Rev. C* **98** (2018) 044902 [arXiv:1710.07864] [INSPIRE].

[17] ATLAS collaboration, *Transverse momentum and process dependent azimuthal anisotropies in* $\sqrt{s_{\rm NN}} = 8.16$ *TeV* $p+Pb$ *collisions with the ATLAS detector*, *Eur. Phys. J. C* **80** (2020) 73 [arXiv:1910.13978] [INSPIRE].

JHEP08(2024)234

[18] ATLAS collaboration, *Observation of Long-Range Elliptic Azimuthal Anisotropies in $\sqrt{s} = 13$ and 2.76 TeV pp Collisions with the ATLAS Detector*, *Phys. Rev. Lett.* **116** (2016) 172301 [arXiv:1509.04776] [INSPIRE].

[19] ATLAS collaboration, *Measurements of long-range azimuthal anisotropies and associated Fourier coefficients for pp collisions at $\sqrt{s} = 5.02$ and 13 TeV and p+Pb collisions at $\sqrt{s_{\rm NN}} = 5.02$ TeV with the ATLAS detector*, *Phys. Rev. C* **96** (2017) 024908 [arXiv:1609.06213] [INSPIRE].

[20] ATLAS collaboration, *Measurement of multi-particle azimuthal correlations in pp, p+Pb and low-multiplicity Pb+Pb collisions with the ATLAS detector*, *Eur. Phys. J. C* **77** (2017) 428 [arXiv:1705.04176] [INSPIRE].

[21] CMS collaboration, *Observation of Correlated Azimuthal Anisotropy Fourier Harmonics in pp and p+Pb Collisions at the LHC*, *Phys. Rev. Lett.* **120** (2018) 092301 [arXiv:1709.09189] [INSPIRE].

[22] ALICE collaboration, *Investigations of Anisotropic Flow Using Multiparticle Azimuthal Correlations in pp, p-Pb, Xe-Xe, and Pb-Pb Collisions at the LHC*, *Phys. Rev. Lett.* **123** (2019) 142301 [arXiv:1903.01790] [INSPIRE].

[23] ATLAS collaboration, *Measurement of azimuthal anisotropy of muons from charm and bottom hadrons in pp collisions at $\sqrt{s} = 13$ TeV with the ATLAS detector*, *Phys. Rev. Lett.* **124** (2020) 082301 [arXiv:1909.01650] [INSPIRE].

[24] ALICE collaboration, *Centrality dependence of particle production in p-Pb collisions at $\sqrt{s_{\rm NN}} = 5.02$ TeV*, *Phys. Rev. C* **91** (2015) 064905 [arXiv:1412.6828] [INSPIRE].

[25] ALICE collaboration, *Measurement of charged jet production cross sections and nuclear modification in p-Pb collisions at $\sqrt{s_{\rm NN}} = 5.02$ TeV*, *Phys. Lett. B* **749** (2015) 68 [arXiv:1503.00681] [INSPIRE].

[26] ALICE collaboration, *Centrality dependence of charged jet production in p-Pb collisions at $\sqrt{s_{\rm NN}} = 5.02$ TeV*, arXiv:1603.03402 [DOI:10.1140/epjc/s10052-016-4107-8] [INSPIRE].

[27] ATLAS collaboration, *Transverse momentum, rapidity, and centrality dependence of inclusive charged-particle production in $\sqrt{s_{\rm NN}} = 5.02$ TeV p+Pb collisions measured by the ATLAS experiment*, *Phys. Lett. B* **763** (2016) 313 [arXiv:1605.06436] [INSPIRE].

[28] ALICE collaboration, *Measurement of electrons from heavy-flavour hadron decays as a function of multiplicity in p-Pb collisions at $\sqrt{s_{\rm NN}} = 5.02$ TeV*, *JHEP* **02** (2020) 077 [arXiv:1910.14399] [INSPIRE].

[29] ALICE collaboration, *Measurement of prompt D^0, D^+, D^{*+}, and D_S^+ production in p-Pb collisions at $\sqrt{s_{\rm NN}} = 5.02$ TeV*, *JHEP* **12** (2019) 092 [arXiv:1906.03425] [INSPIRE].

[30] K. Dusling and R. Venugopalan, *Evidence for BFKL and saturation dynamics from dihadron spectra at the LHC*, *Phys. Rev. D* **87** (2013) 051502 [arXiv:1210.3890] [INSPIRE].

[31] K. Dusling and R. Venugopalan, *Comparison of the color glass condensate to dihadron correlations in proton-proton and proton-nucleus collisions*, *Phys. Rev. D* **87** (2013) 094034 [arXiv:1302.7018] [INSPIRE].

[32] K. Dusling, W. Li and B. Schenke, *Novel collective phenomena in high-energy proton-proton and proton-nucleus collisions*, *Int. J. Mod. Phys. E* **25** (2016) 1630002 [arXiv:1509.07939] [INSPIRE].

[33] C. Zhang et al., *Collectivity of heavy mesons in proton-nucleus collisions*, *Phys. Rev. D* **102** (2020) 034010 [arXiv:2002.09878] [INSPIRE].

JHEP08(2024)234

[34] L. He, T. Edmonds, Z.-W. Lin, F. Liu, D. Molnar and F. Wang, *Anisotropic parton escape is the dominant source of azimuthal anisotropy in transport models*, *Phys. Lett. B* **753** (2016) 506 [arXiv:1502.05572] [INSPIRE].

[35] ALICE collaboration, *Azimuthal anisotropy of charged jet production in* $\sqrt{s_{\rm NN}} = 2.76$ *TeV Pb-Pb collisions*, *Phys. Lett. B* **753** (2016) 511 [arXiv:1509.07334] [INSPIRE].

[36] Z.-W. Lin, C.M. Ko, B.-A. Li, B. Zhang and S. Pal, *A Multi-phase transport model for relativistic heavy ion collisions*, *Phys. Rev. C* **72** (2005) 064901 [nucl-th/0411110] [INSPIRE].

[37] H. Li, Z.-W. Lin and F. Wang, *Charm quarks are more hydrodynamic than light quarks in final-state elliptic flow*, *Phys. Rev. C* **99** (2019) 044911 [arXiv:1804.02681] [INSPIRE].

[38] ALICE collaboration, *The ALICE experiment at the CERN LHC*, 2008 *JINST* **3** S08002 [INSPIRE].

[39] ALICE collaboration, *Performance of the ALICE Experiment at the CERN LHC*, *Int. J. Mod. Phys. A* **29** (2014) 1430044 [arXiv:1402.4476] [INSPIRE].

[40] J. Alme et al., *The ALICE TPC, a large 3-dimensional tracking device with fast readout for ultra-high multiplicity events*, *Nucl. Instrum. Meth. A* **622** (2010) 316 [arXiv:1001.1950] [INSPIRE].

[41] ALICE collaboration, *Alignment of the ALICE Inner Tracking System with cosmic-ray tracks*, 2010 *JINST* **5** P03003 [arXiv:1001.0502] [INSPIRE].

[42] ALICE collaboration, *ALICE Inner Tracking System (ITS): Technical Design Report*, CERN-LHCC-99-012 (1999).

[43] ALICE collaboration, *ALICE forward detectors: FMD, TO and VO: Technical Design Report*, CERN-LHCC-2004-025 (2004).

[44] ALICE collaboration, *Performance of the ALICE VZERO system*, 2013 *JINST* **8** P10016 [arXiv:1306.3130] [INSPIRE].

[45] ALICE collaboration, *Centrality determination in heavy ion collisions*, ALICE-PUBLIC-2018-011 (2018).

[46] ALICE collaboration, *Transverse momentum spectra and nuclear modification factors of charged particles in pp, p-Pb and Pb-Pb collisions at the LHC*, *JHEP* **11** (2018) 013 [arXiv:1802.09145] [INSPIRE].

[47] ALICE collaboration, *Energy dependence and fluctuations of anisotropic flow in Pb-Pb collisions at* $\sqrt{s_{\rm NN}} = 5.02$ *and* 2.76 *TeV*, *JHEP* **07** (2018) 103 [arXiv:1804.02944] [INSPIRE].

[48] ALICE collaboration, *Supplemental material: Azimuthal anisotropy of jet particles in p-Pb and Pb-Pb collisions at* $\sqrt{s_{\rm NN}} = 5.02$ *TeV*, ALICE-PUBLIC-2022-020 (2022).

[49] ALICE collaboration, *Measurements of azimuthal anisotropies at forward and backward rapidity with muons in high-multiplicity p-Pb collisions at* $\sqrt{s_{\rm NN}} = 8.16$ *TeV*, *Phys. Lett. B* **846** (2023) 137782 [arXiv:2210.08980] [INSPIRE].

[50] ALICE collaboration, *Long-range angular correlations on the near and away side in p-Pb collisions at* $\sqrt{s_{\rm NN}} = 5.02$ *TeV*, *Phys. Lett. B* **719** (2013) 29 [arXiv:1212.2001] [INSPIRE].

[51] ALICE collaboration, *Multiplicity dependence of jet-like two-particle correlation structures in p-Pb collisions at* $\sqrt{s_{\rm NN}} = 5.02$ *TeV*, *Phys. Lett. B* **741** (2015) 38 [arXiv:1406.5463] [INSPIRE].

[52] ALICE collaboration, *Forward-central two-particle correlations in p-Pb collisions at* $\sqrt{s_{\rm NN}} = 5.02$ *TeV*, *Phys. Lett. B* **753** (2016) 126 [arXiv:1506.08032] [INSPIRE].

JHEP08(2024)234

[53] M. Luzum and J.-Y. Ollitrault, *Eliminating experimental bias in anisotropic-flow measurements of high-energy nuclear collisions*, *Phys. Rev. C* **87** (2013) 044907 [arXiv:1209.2323] [INSPIRE].

[54] ALICE collaboration, *Measurements of long-range two-particle correlation over a wide pseudorapidity range in p-Pb collisions at* $\sqrt{s_{\rm NN}} = 5.0$ *TeV*, *JHEP* **01** (2024) 199 [arXiv:2308.16590] [INSPIRE].

[55] STAR collaboration, *Elliptic flow from two and four particle correlations in Au+Au collisions at* $\sqrt{s_{\rm NN}} = 130$ *GeV*, *Phys. Rev. C* **66** (2002) 034904 [nucl-ex/0206001] [INSPIRE].

[56] S.A. Voloshin, A.M. Poskanzer and R. Snellings, *Collective phenomena in non-central nuclear collisions*, *Landolt-Bornstein* **23** (2010) 293 [arXiv:0809.2949] [INSPIRE].

[57] I. Selyuzhenkov and S.A. Voloshin, *Effects of non-uniform acceptance in anisotropic flow measurement*, *Phys. Rev. C* **77** (2008) 034904 [arXiv:0707.4672] [INSPIRE].

[58] ALICE collaboration, *Anisotropic flow of identified particles in Pb-Pb collisions at* $\sqrt{s_{\rm NN}} = 5.02$ *TeV*, *JHEP* **09** (2018) 006 [arXiv:1805.04390] [INSPIRE].

[59] ALICE collaboration, *J/ψ Elliptic Flow in Pb-Pb Collisions at* $\sqrt{s_{\rm NN}} = 2.76$ *TeV*, *Phys. Rev. Lett.* **111** (2013) 162301 [arXiv:1303.5880] [INSPIRE].

[60] Z.-W. Lin and L. Zheng, *Further developments of a multi-phase transport model for relativistic nuclear collisions*, *Nucl. Sci. Tech.* **32** (2021) 113 [arXiv:2110.02989] [INSPIRE].

[61] C. Loizides, J. Kamin and D. d'Enterria, *Improved Monte Carlo Glauber predictions at present and future nuclear colliders*, *Phys. Rev. C* **97** (2018) 054910 [*Erratum ibid.* **99** (2019) 019901] [arXiv:1710.07098] [INSPIRE].

[62] H.-S. Wang and G.-L. Ma, *Testing the collectivity in large and small colliding systems with test particles*, *Phys. Rev. C* **106** (2022) 064907 [arXiv:2208.06854] [INSPIRE].

[63] X.-N. Wang and M. Gyulassy, *HIJING: A Monte Carlo model for multiple jet production in pp, pA and AA collisions*, *Phys. Rev. D* **44** (1991) 3501 [INSPIRE].

[64] M. Gyulassy and X.-N. Wang, *HIJING 1.0: A Monte Carlo program for parton and particle production in high-energy hadronic and nuclear collisions*, *Comput. Phys. Commun.* **83** (1994) 307 [nucl-th/9502021] [INSPIRE].

[65] B. Zhang, *ZPC 1.0.1: A Parton cascade for ultrarelativistic heavy ion collisions*, *Comput. Phys. Commun.* **109** (1998) 193 [nucl-th/9709009] [INSPIRE].

[66] B.-A. Li and C.M. Ko, *Formation of superdense hadronic matter in high-energy heavy ion collisions*, *Phys. Rev. C* **52** (1995) 2037 [nucl-th/9505016] [INSPIRE].

[67] S.-Y. Tang, L. Zheng, X.-M. Zhang and R.-Z. Wan, *Investigating the elliptic anisotropy of identified particles in p-Pb collisions with a multi-phase transport model*, *Nucl. Sci. Tech.* **35** (2024) 32 [arXiv:2303.06577] [INSPIRE].

[68] ALICE collaboration, *Multiplicity dependence of charged pion, kaon, and (anti)proton production at large transverse momentum in p-Pb collisions at* $\sqrt{s_{\rm NN}} = 5.02$ *TeV*, *Phys. Lett. B* **760** (2016) 720 [arXiv:1601.03658] [INSPIRE].

JHEP08(2024)234

The ALICE collaboration

S. Acharya[126], D. Adamová[86], A. Adler[70], G. Aglieri Rinella[32], M. Agnello[29], N. Agrawal[51], Z. Ahammed[134], S. Ahmad[15], S.U. Ahn[71], I. Ahuja[37], A. Akindinov[140], M. Al-Turany[97], D. Aleksandrov[140], B. Alessandro[56], H.M. Alfanda[6], R. Alfaro Molina[67], B. Ali[15], A. Alici[25], N. Alizadehvandchali[115], A. Alkin[32], J. Alme[20], G. Alocco[52], T. Alt[64], I. Altsybeev[140], J.R. Alvarado[44], M.N. Anaam[6], C. Andrei[45], A. Andronic[125], V. Anguelov[94], F. Antinori[54], P. Antonioli[51], N. Apadula[74], L. Aphecetche[103], H. Appelshäuser[64], C. Arata[73], S. Arcelli[25], M. Aresti[52], R. Arnaldi[56], J.G.M.C.A. Arneiro[110], I.C. Arsene[19], M. Arslandok[137], A. Augustinus[32], R. Averbeck[97], M.D. Azmi[15], A. Badalà[53], J. Bae[104], Y.W. Baek[40], X. Bai[119], R. Bailhache[64], Y. Bailung[48], A. Balbino[29], A. Baldisseri[129], B. Balis[2], D. Banerjee[4], Z. Banoo[91], R. Barbera[26], F. Barile[31], L. Barioglio[95], M. Barlou[78], G.G. Barnaföldi[46], L.S. Barnby[85], V. Barret[126], L. Barreto[110], C. Bartels[118], K. Barth[32], E. Bartsch[64], N. Bastid[126], S. Basu[75], G. Batigne[103], D. Battistini[95], B. Batyunya[141], D. Bauri[47], J.L. Bazo Alba[101], I.G. Bearden[83], C. Beattie[137], P. Becht[97], D. Behera[48], I. Belikov[128], A.D.C. Bell Hechavarria[125], F. Bellini[25], R. Bellwied[115], S. Belokurova[140], V. Belyaev[140], G. Bencedi[46], S. Beole[24], Y. Berdnikov[140], A. Berdnikova[94], L. Bergmann[94], M.G. Besoiu[63], L. Betev[32], P.P. Bhaduri[134], A. Bhasin[91], M.A. Bhat[4], B. Bhattacharjee[41], L. Bianchi[24], N. Bianchi[49], J. Bielčík[35], J. Bielčíková[86], J. Biernat[107], A.P. Bigot[128], A. Bilandzic[95], G. Biro[46], S. Biswas[4], N. Bize[103], J.T. Blair[108], D. Blau[140], M.B. Blidaru[97], N. Bluhme[38], C. Blume[64], G. Boca[21,55], F. Bock[87], T. Bodova[20], A. Bogdanov[140], S. Boi[22], J. Bok[58], L. Boldizsár[46], M. Bombara[37], P.M. Bond[32], G. Bonomi[133,55], H. Borel[129], A. Borissov[140], A.G. Borquez Carcamo[94], H. Bossi[137], E. Botta[24], Y.E.M. Bouziani[64], L. Bratrud[64], P. Braun-Munzinger[97], M. Bregant[110], M. Broz[35], G.E. Bruno[96,31], M.D. Buckland[23], D. Budnikov[140], H. Buesching[64], S. Bufalino[29], O. Bugnon[103], P. Buhler[102], Z. Buthelezi[68,122], S.A. Bysiak[107], M. Cai[6], H. Caines[137], A. Caliva[97], E. Calvo Villar[101], J.M.M. Camacho[109], P. Camerini[23], F.D.M. Canedo[110], S.L. Cantway[137], M. Carabas[113], A.A. Carballo[32], F. Carnesecchi[32], R. Caron[127], L.A.D. Carvalho[110], J. Castillo Castellanos[129], F. Catalano[24], C. Ceballos Sanchez[141], I. Chakaberia[74], P. Chakraborty[47], S. Chandra[134], S. Chapeland[32], M. Chartier[118], S. Chattopadhyay[134], S. Chattopadhyay[99], T. Cheng[97,6], C. Cheshkov[127], B. Cheynis[127], V. Chibante Barroso[32], D.D. Chinellato[111], E.S. Chizzali[II,95], J. Cho[58], S. Cho[58], P. Chochula[32], P. Christakoglou[84], C.H. Christensen[83], P. Christiansen[75], T. Chujo[124], M. Ciacco[29], C. Cicalo[52], F. Cindolo[51], M.R. Ciupek[97], G. Clai[III,51], F. Colamaria[50], J.S. Colburn[100], D. Colella[96,31], M. Colocci[25], M. Concas[56], G. Conesa Balbastre[73], Z. Conesa del Valle[130], G. Contin[23], J.G. Contreras[35], M.L. Coquet[129], T.M. Cormier[I,87], P. Cortese[132,56], M.R. Cosentino[112], F. Costa[32], S. Costanza[21,55], C. Cot[130], J. Crkovská[94], P. Crochet[126], R. Cruz-Torres[74], E. Cuautle[65], P. Cui[6], A. Dainese[54], M.C. Danisch[94], A. Danu[63], P. Das[80], P. Das[4], S. Das[4], A.R. Dash[125], S. Dash[47], A. De Caro[28], G. de Cataldo[50], J. de Cuveland[38], A. De Falco[22], D. De Gruttola[28], N. De Marco[56], C. De Martin[23], S. De Pasquale[28], R. Deb[133], S. Deb[48], R.J. Debski[2], K.R. Deja[135], R. Del Grande[95], L. Dello Stritto[28], W. Deng[6], P. Dhankher[18], D. Di Bari[31],

JHEP08(2024)234

A. Di Mauro[32], R.A. Diaz[141,7], T. Dietel[114], Y. Ding[127,6], R. Divià[32], D.U. Dixit[18], Ø. Djuvsland[20], U. Dmitrieva[140], A. Dobrin[63], B. Dönigus[64], J.M. Dubinski[135], A. Dubla[97], S. Dudi[90], P. Dupieux[126], M. Durkac[106], N. Dzalaiova[12], T.M. Eder[125], R.J. Ehlers[87], V.N. Eikeland[20], F. Eisenhut[64], D. Elia[50], B. Erazmus[103], F. Ercolessi[25], F. Erhardt[89], M.R. Ersdal[20], B. Espagnon[130], G. Eulisse[32], D. Evans[100], S. Evdokimov[140], L. Fabbietti[95], M. Faggin[27], J. Faivre[73], F. Fan[6], W. Fan[74], A. Fantoni[49], M. Fasel[87], P. Fecchio[29], A. Feliciello[56], G. Feofilov[140], A. Fernández Téllez[44], L. Ferrandi[110], M.B. Ferrer[32], A. Ferrero[129], C. Ferrero[IV,56], A. Ferretti[24], V.J.G. Feuillard[94], V. Filova[35], D. Finogeev[140], F.M. Fionda[52], F. Flor[115], A.N. Flores[108], S. Foertsch[68], I. Fokin[94], S. Fokin[140], E. Fragiacomo[57], E. Frajna[46], U. Fuchs[32], N. Funicello[28], C. Furget[73], A. Furs[140], T. Fusayasu[98], J.J. Gaardhøje[83], M. Gagliardi[24], A.M. Gago[101], C.D. Galvan[109], D.R. Gangadharan[115], P. Ganoti[78], C. Garabatos[97], T. García Chávez[44], E. Garcia-Solis[9], K. Garg[103], C. Gargiulo[32], K. Garner[125], P. Gasik[97], A. Gautam[117], M.B. Gay Ducati[66], M. Germain[103], A. Ghimouz[124], C. Ghosh[134], M. Giacalone[51,25], P. Giubellino[97,56], P. Giubilato[27], A.M.C. Glaenzer[129], P. Glässel[94], E. Glimos[121], D.J.Q. Goh[76], V. Gonzalez[136], L.H. González-Trueba[67], M. Gorgon[2], S. Gotovac[33], V. Grabski[67], L.K. Graczykowski[135], E. Grecka[86], A. Grelli[59], C. Grigoras[32], V. Grigoriev[140], S. Grigoryan[141,1], F. Grosa[32], J.F. Grosse-Oetringhaus[32], R. Grosso[97], D. Grund[35], G.G. Guardiano[111], R. Guernane[73], M. Guilbaud[103], K. Gulbrandsen[83], T. Gündem[64], T. Gunji[123], W. Guo[6], A. Gupta[91], R. Gupta[91], L. Gyulai[46], M.K. Habib[97], C. Hadjidakis[130], F.U. Haider[91], H. Hamagaki[76], A. Hamdi[74], M. Hamid[6], Y. Han[138], R. Hannigan[108], M.R. Haque[135], J.W. Harris[137], A. Harton[9], H. Hassan[87], D. Hatzifotiadou[51], P. Hauer[42], L.B. Havener[137], S.T. Heckel[95], E. Hellbär[97], H. Helstrup[34], M. Hemmer[64], T. Herman[35], G. Herrera Corral[8], F. Herrmann[125], S. Herrmann[127], K.F. Hetland[34], B. Heybeck[64], H. Hillemanns[32], C. Hills[118], B. Hippolyte[128], F.W. Hoffmann[70], B. Hofman[59], B. Hohlweger[84], G.H. Hong[138], M. Horst[95], A. Horzyk[2], Y. Hou[6], P. Hristov[32], C. Hughes[121], P. Huhn[64], L.M. Huhta[116], T.J. Humanic[88], A. Hutson[115], D. Hutter[38], J.P. Iddon[118], R. Ilkaev[140], H. Ilyas[13], M. Inaba[124], G.M. Innocenti[32], M. Ippolitov[140], A. Isakov[86], T. Isidori[117], M.S. Islam[99], M. Ivanov[97], M. Ivanov[12], V. Ivanov[140], M. Jablonski[2], B. Jacak[74], N. Jacazio[32], P.M. Jacobs[74], S. Jadlovska[106], J. Jadlovsky[106], S. Jaelani[82], L. Jaffe[38], C. Jahnke[111], M.J. Jakubowska[135], M.A. Janik[135], T. Janson[70], M. Jercic[89], S. Jia[10], A.A.P. Jimenez[65], F. Jonas[87,125], J.M. Jowett[32,97], J. Jung[64], M. Jung[64], A. Junique[32], A. Jusko[100], J. Kaewjai[105], P. Kalinak[60], A.S. Kalteyer[97], A. Kalweit[32], V. Kaplin[140], A. Karasu Uysal[V,72], D. Karatovic[89], O. Karavichev[140], T. Karavicheva[140], P. Karczmarczyk[135], E. Karpechev[140], M.J. Karwowska[32,135], U. Kebschull[70], R. Keidel[139], D.L.D. Keijdener[59], M. Keil[32], B. Ketzer[42], A.M. Khan[6], S. Khan[15], A. Khanzadeev[140], Y. Kharlov[140], A. Khatun[117,15], A. Khuntia[107], M.B. Kidson[114], B. Kileng[34], B. Kim[16], C. Kim[16], D.J. Kim[116], E.J. Kim[69], J. Kim[138], J.S. Kim[40], J. Kim[69], M. Kim[18,94], S. Kim[17], T. Kim[138], K. Kimura[92], S. Kirsch[64], I. Kisel[38], S. Kiselev[140], A. Kisiel[135], J.P. Kitowski[2], J.L. Klay[5], J. Klein[32], S. Klein[74], C. Klein-Bösing[125], M. Kleiner[64], T. Klemenz[95], A. Kluge[32], A.G. Knospe[115], C. Kobdaj[105], T. Kollegger[97], A. Kondratyev[141], N. Kondratyeva[140], E. Kondratyuk[140], J. Konig[64], S.A. Konigstorfer[95],

JHEP08(2024)234

P.J. Konopka[32], G. Kornakov[135], M. Korwieser[95], S.D. Koryciak[2], A. Kotliarov[86], V. Kovalenko[140], M. Kowalski[107], V. Kozhuharov[36], I. Králik[60], A. Kravčáková[37], L. Krcal[32,38], L. Kreis[97], M. Krivda[100,60], F. Krizek[86], K. Krizkova Gajdosova[35], M. Kroesen[94], M. Krüger[64], D.M. Krupova[35], E. Kryshen[140], V. Kučera[32], C. Kuhn[128], P.G. Kuijer[84], T. Kumaoka[124], D. Kumar[134], L. Kumar[90], N. Kumar[90], S. Kumar[31], S. Kundu[32], P. Kurashvili[79], A. Kurepin[140], A.B. Kurepin[140], A. Kuryakin[140], S. Kushpil[86], J. Kvapil[100], M.J. Kweon[58], J.Y. Kwon[58], Y. Kwon[138], S.L. La Pointe[38], P. La Rocca[26], Y.S. Lai[74], A. Lakrathok[105], M. Lamanna[32], R. Langoy[120], P. Larionov[32], E. Laudi[32], L. Lautner[32,95], R. Lavicka[102], T. Lazareva[140], R. Lea[133,55], H. Lee[104], G. Legras[125], J. Lehrbach[38], T.M. Lelek[2], R.C. Lemmon[85], I. León Monzón[109], M.M. Lesch[95], E.D. Lesser[18], M. Lettrich[95], P. Lévai[46], X. Li[10], X.L. Li[6], J. Lien[120], R. Lietava[100], I. Likmeta[115], B. Lim[24,16], S.H. Lim[16], V. Lindenstruth[38], A. Lindner[45], C. Lippmann[97], A. Liu[18], D.H. Liu[6], J. Liu[118], I.M. Lofnes[20], C. Loizides[87], S. Lokos[107], J. Lömker[59], P. Loncar[33], J.A. Lopez[94], X. Lopez[126], E. López Torres[7], P. Lu[97,119], J.R. Luhder[125], M. Lunardon[27], G. Luparello[57], Y.G. Ma[39], A. Maevskaya[140], M. Mager[32], T. Mahmoud[42], A. Maire[128], M.V. Makariev[36], M. Malaev[140], G. Malfattore[25], N.M. Malik[91], Q.W. Malik[19], S.K. Malik[91], L. Malinina[I,VIII,141], D. Mal'Kevich[140], D. Mallick[80], N. Mallick[48], G. Mandaglio[30,53], S.K. Mandal[79], V. Manko[140], F. Manso[126], V. Manzari[50], Y. Mao[6], G.V. Margagliotti[23], A. Margotti[51], A. Marín[97], C. Markert[108], P. Martinengo[32], J.L. Martinez[115], M.I. Martínez[44], G. Martínez García[103], S. Masciocchi[97], M. Masera[24], A. Masoni[52], L. Massacrier[130], A. Mastroserio[131,50], O. Matonoha[75], P.F.T. Matuoka[110], A. Matyja[107], C. Mayer[107], A.L. Mazuecos[32], F. Mazzaschi[24], M. Mazzilli[32], J.E. Mdhluli[122], A.F. Mechler[64], Y. Melikyan[43,140], A. Menchaca-Rocha[67], E. Meninno[102], A.S. Menon[115], M. Meres[12], S. Mhlanga[114,68], Y. Miake[124], L. Micheletti[56], L.C. Migliorin[127], D.L. Mihaylov[95], K. Mikhaylov[141,140], A.N. Mishra[46], D. Miśkowiec[97], A. Modak[4], A.P. Mohanty[59], B. Mohanty[80], M. Mohisin Khan[VI,15], M.A. Molander[43], Z. Moravcova[83], C. Mordasini[95], D.A. Moreira De Godoy[125], I. Morozov[140], A. Morsch[32], T. Mrnjavac[32], V. Muccifora[49], S. Muhuri[134], J.D. Mulligan[74], A. Mulliri[22], M.G. Munhoz[110], R.H. Munzer[64], H. Murakami[123], S. Murray[114], L. Musa[32], J. Musinsky[60], J.W. Myrcha[135], B. Naik[122], A.I. Nambrath[18], B.K. Nandi[47], R. Nania[51], E. Nappi[50], A.F. Nassirpour[75], A. Nath[94], C. Nattrass[121], M.N. Naydenov[36], A. Neagu[19], A. Negru[113], L. Nellen[65], S.V. Nesbo[34], G. Neskovic[38], D. Nesterov[140], B.S. Nielsen[83], E.G. Nielsen[83], S. Nikolaev[140], S. Nikulin[140], V. Nikulin[140], F. Noferini[51], S. Noh[11], P. Nomokonov[141], J. Norman[118], N. Novitzky[124], P. Nowakowski[135], A. Nyanin[140], J. Nystrand[20], M. Ogino[76], A. Ohlson[75], V.A. Okorokov[140], J. Oleniacz[135], A.C. Oliveira Da Silva[121], M.H. Oliver[137], A. Onnerstad[116], C. Oppedisano[56], A. Ortiz Velasquez[65], J. Otwinowski[107], M. Oya[92], K. Oyama[76], Y. Pachmayer[94], S. Padhan[47], D. Pagano[133,55], G. Paić[65], S. Paisano-Guzmán[44], A. Palasciano[50], S. Panebianco[129], H. Park[124], H. Park[104], J. Park[58], J.E. Parkkila[32], R.N. Patra[91], B. Paul[22], H. Pei[6], T. Peitzmann[59], X. Peng[6], M. Pennisi[24], L.G. Pereira[66], D. Peresunko[140], G.M. Perez[7], S. Perrin[129], Y. Pestov[140], V. Petráček[35], V. Petrov[140], M. Petrovici[45], R.P. Pezzi[103,66], S. Piano[57], M. Pikna[12], P. Pillot[103], O. Pinazza[51,32], L. Pinsky[115], C. Pinto[95], S. Pisano[49], M. Płoskoń[74],

JHEP08(2024)234

M. Planinic[89], F. Pliquett[64], M.G. Poghosyan[87], B. Polichtchouk[140], S. Politano[29], N. Poljak[89], A. Pop[45], S. Porteboeuf-Houssais[126], V. Pozdniakov[141], K.K. Pradhan[48], S.K. Prasad[4], S. Prasad[48], R. Preghenella[51], F. Prino[56], C.A. Pruneau[136], I. Pshenichnov[140], M. Puccio[32], S. Pucillo[24], Z. Pugelova[106], S. Qiu[84], L. Quaglia[24], R.E. Quishpe[115], S. Ragoni[14], A. Rakotozafindrabe[129], L. Ramello[132,56], F. Rami[128], T.A. Rancien[73], M. Rasa[26], S.S. Räsänen[43], R. Rath[51], M.P. Rauch[20], I. Ravasenga[84], K.F. Read[87,121], C. Reckziegel[112], A.R. Redelbach[38], K. Redlich[VII,79], C.A. Reetz[97], H.D. Regules-Medel[44], A. Rehman[20], F. Reidt[32], H.A. Reme-Ness[34], Z. Rescakova[37], K. Reygers[94], A. Riabov[140], V. Riabov[140], R. Ricci[28], M. Richter[19], A.A. Riedel[95], W. Riegler[32], C. Ristea[63], M. Rodríguez Cahuantzi[44], S.A. Rodríguez Ramírez[44], K. Røed[19], R. Rogalev[140], E. Rogochaya[141], T.S. Rogoschinski[64], D. Rohr[32], D. Röhrich[20], P.F. Rojas[44], S. Rojas Torres[35], P.S. Rokita[135], G. Romanenko[141], F. Ronchetti[49], A. Rosano[30,53], E.D. Rosas[65], K. Roslon[135], A. Rossi[54], A. Roy[48], S. Roy[47], N. Rubini[25], D. Ruggiano[135], R. Rui[23], B. Rumyantsev[141], P.G. Russek[2], R. Russo[84], A. Rustamov[81], E. Ryabinkin[140], Y. Ryabov[140], A. Rybicki[107], H. Rytkonen[116], W. Rzesa[135], O.A.M. Saarimaki[43], R. Sadek[103], S. Sadhu[31], S. Sadovsky[140], J. Saetre[20], K. Šafařík[35], S.K. Saha[4], S. Saha[80], B. Sahoo[47], R. Sahoo[48], S. Sahoo[61], D. Sahu[48], P.K. Sahu[61], J. Saini[134], K. Sajdakova[37], S. Sakai[124], M.P. Salvan[97], S. Sambyal[91], I. Sanna[32,95], T.B. Saramela[110], D. Sarkar[136], N. Sarkar[134], P. Sarma[41], V. Sarritzu[22], V.M. Sarti[95], M.H.P. Sas[137], J. Schambach[87], H.S. Scheid[64], C. Schiaua[45], R. Schicker[94], A. Schmah[94], C. Schmidt[97], H.R. Schmidt[93], M.O. Schmidt[32], M. Schmidt[93], N.V. Schmidt[87], A.R. Schmier[121], R. Schotter[128], A. Schröter[38], J. Schukraft[32], K. Schwarz[97], K. Schweda[97], G. Scioli[25], E. Scomparin[56], J.E. Seger[14], Y. Sekiguchi[123], D. Sekihata[123], I. Selyuzhenkov[97,140], S. Senyukov[128], J.J. Seo[58], D. Serebryakov[140], L. Šerkšnytė[95], A. Sevcenco[63], T.J. Shaba[68], A. Shabetai[103], R. Shahoyan[32], A. Shangaraev[140], A. Sharma[90], B. Sharma[91], D. Sharma[47], H. Sharma[107], M. Sharma[91], S. Sharma[76], S. Sharma[91], U. Sharma[91], A. Shatat[130], O. Sheibani[115], K. Shigaki[92], M. Shimomura[77], J. Shin[11], S. Shirinkin[140], Q. Shou[39], Y. Sibiriak[140], S. Siddhanta[52], T. Siemiarczuk[79], T.F. Silva[110], D. Silvermyr[75], T. Simantathammakul[105], R. Simeonov[36], B. Singh[91], B. Singh[95], R. Singh[80], R. Singh[91], R. Singh[48], S. Singh[15], V.K. Singh[134], V. Singhal[134], T. Sinha[99], B. Sitar[12], M. Sitta[132,56], T.B. Skaali[19], G. Skorodumovs[94], M. Slupecki[43], N. Smirnov[137], R.J.M. Snellings[59], E.H. Solheim[19], J. Song[115], A. Songmoolnak[105], F. Soramel[27], R. Spijkers[84], I. Sputowska[107], J. Staa[75], J. Stachel[94], I. Stan[63], P.J. Steffanic[121], S.F. Stiefelmaier[94], D. Stocco[103], I. Storehaug[19], P. Stratmann[125], S. Strazzi[25], C.P. Stylianidis[84], A.A.P. Suaide[110], C. Suire[130], M. Sukhanov[140], M. Suljic[32], R. Sultanov[140], V. Sumberia[91], S. Sumowidagdo[82], S. Swain[61], I. Szarka[12], M. Szymkowski[135], S.F. Taghavi[95], G. Taillepied[97], J. Takahashi[111], G.J. Tambave[20], S. Tang[126,6], Z. Tang[119], J.D. Tapia Takaki[117], N. Tapus[113], L.A. Tarasovicova[125], M.G. Tarzila[45], G.F. Tassielli[31], A. Tauro[32], G. Tejeda Muñoz[44], A. Telesca[32], L. Terlizzi[24], C. Terrevoli[115], G. Tersimonov[3], S. Thakur[4], D. Thomas[108], A. Tikhonov[140], A.R. Timmins[115], M. Tkacik[106], T. Tkacik[106], A. Toia[64], R. Tokumoto[92], N. Topilskaya[140], M. Toppi[49], F. Torales-Acosta[18], T. Tork[130], A.G. Torres Ramos[31], A. Trifiró[30,53], A.S. Triolo[30,53], S. Tripathy[51], T. Tripathy[47],

JHEP08(2024)234

S. Trogolo[32], V. Trubnikov[3], W.H. Trzaska[116], T.P. Trzcinski[135], A. Tumkin[140], R. Turrisi[54], T.S. Tveter[19], K. Ullaland[20], B. Ulukutlu[95], A. Uras[127], M. Urioni[55,133], G.L. Usai[22], M. Vala[37], N. Valle[21], L.V.R. van Doremalen[59], C. Van Hulse[130], M. van Leeuwen[84], C.A. van Veen[94], R.J.G. van Weelden[84], P. Vande Vyvre[32], D. Varga[46], Z. Varga[46], M. Vasileiou[78], A. Vasiliev[140], O. Vázquez Doce[49], O. Vazquez Rueda[115,75], V. Vechernin[140], E. Vercellin[24], S. Vergara Limón[44], L. Vermunt[97], R. Vértesi[46], M. Verweij[59], L. Vickovic[33], Z. Vilakazi[122], O. Villalobos Baillie[100], A. Villani[23], G. Vino[50], A. Vinogradov[140], T. Virgili[28], M.M.O. Virta[116], V. Vislavicius[75], A. Vodopyanov[141], B. Volkel[32], M.A. Völkl[94], K. Voloshin[140], S.A. Voloshin[136], G. Volpe[31], B. von Haller[32], I. Vorobyev[95], N. Vozniuk[140], J. Vrláková[37], C. Wang[39], D. Wang[39], Y. Wang[39], A. Wegrzynek[32], F.T. Weiglhofer[38], S.C. Wenzel[32], J.P. Wessels[125], J. Wiechula[64], J. Wikne[19], G. Wilk[79], J. Wilkinson[97], G.A. Willems[125], B. Windelband[94], M. Winn[129], J.R. Wright[108], W. Wu[39], Y. Wu[119], R. Xu[6], A. Yadav[42], A.K. Yadav[134], S. Yalcin[72], Y. Yamaguchi[92], S. Yang[20], S. Yano[92], Z. Yin[6], I.-K. Yoo[16], J.H. Yoon[58], S. Yuan[20], A. Yuncu[94], V. Zaccolo[23], C. Zampolli[32], F. Zanone[94], N. Zardoshti[32,100], A. Zarochentsev[140], P. Závada[62], N. Zaviyalov[140], M. Zhalov[140], B. Zhang[6], L. Zhang[39], M. Zhang[6], S. Zhang[39], X. Zhang[6], Y. Zhang[119], Z. Zhang[6], M. Zhao[10], V. Zherebchevskii[140], Y. Zhi[10], D. Zhou[6], Y. Zhou[83], J. Zhu[97,6], Y. Zhu[6], S.C. Zugravel[56], N. Zurlo[133,55]

[1] *A.I. Alikhanyan National Science Laboratory (Yerevan Physics Institute) Foundation, Yerevan, Armenia*
[2] *AGH University of Krakow, Cracow, Poland*
[3] *Bogolyubov Institute for Theoretical Physics, National Academy of Sciences of Ukraine, Kiev, Ukraine*
[4] *Bose Institute, Department of Physics and Centre for Astroparticle Physics and Space Science (CAPSS), Kolkata, India*
[5] *California Polytechnic State University, San Luis Obispo, California, United States*
[6] *Central China Normal University, Wuhan, China*
[7] *Centro de Aplicaciones Tecnológicas y Desarrollo Nuclear (CEADEN), Havana, Cuba*
[8] *Centro de Investigación y de Estudios Avanzados (CINVESTAV), Mexico City and Mérida, Mexico*
[9] *Chicago State University, Chicago, Illinois, United States*
[10] *China Institute of Atomic Energy, Beijing, China*
[11] *Chungbuk National University, Cheongju, Republic of Korea*
[12] *Comenius University Bratislava, Faculty of Mathematics, Physics and Informatics, Bratislava, Slovak Republic*
[13] *COMSATS University Islamabad, Islamabad, Pakistan*
[14] *Creighton University, Omaha, Nebraska, United States*
[15] *Department of Physics, Aligarh Muslim University, Aligarh, India*
[16] *Department of Physics, Pusan National University, Pusan, Republic of Korea*
[17] *Department of Physics, Sejong University, Seoul, Republic of Korea*
[18] *Department of Physics, University of California, Berkeley, California, United States*
[19] *Department of Physics, University of Oslo, Oslo, Norway*
[20] *Department of Physics and Technology, University of Bergen, Bergen, Norway*
[21] *Dipartimento di Fisica, Università di Pavia, Pavia, Italy*
[22] *Dipartimento di Fisica dell'Università and Sezione INFN, Cagliari, Italy*
[23] *Dipartimento di Fisica dell'Università and Sezione INFN, Trieste, Italy*
[24] *Dipartimento di Fisica dell'Università and Sezione INFN, Turin, Italy*
[25] *Dipartimento di Fisica e Astronomia dell'Università and Sezione INFN, Bologna, Italy*
[26] *Dipartimento di Fisica e Astronomia dell'Università and Sezione INFN, Catania, Italy*
[27] *Dipartimento di Fisica e Astronomia dell'Università and Sezione INFN, Padova, Italy*

JHEP08(2024)234

[28] *Dipartimento di Fisica 'E.R. Caianiello' dell'Università and Gruppo Collegato INFN, Salerno, Italy*
[29] *Dipartimento DISAT del Politecnico and Sezione INFN, Turin, Italy*
[30] *Dipartimento di Scienze MIFT, Università di Messina, Messina, Italy*
[31] *Dipartimento Interateneo di Fisica 'M. Merlin' and Sezione INFN, Bari, Italy*
[32] *European Organization for Nuclear Research (CERN), Geneva, Switzerland*
[33] *Faculty of Electrical Engineering, Mechanical Engineering and Naval Architecture, University of Split, Split, Croatia*
[34] *Faculty of Engineering and Science, Western Norway University of Applied Sciences, Bergen, Norway*
[35] *Faculty of Nuclear Sciences and Physical Engineering, Czech Technical University in Prague, Prague, Czech Republic*
[36] *Faculty of Physics, Sofia University, Sofia, Bulgaria*
[37] *Faculty of Science, P.J. Šafárik University, Košice, Slovak Republic*
[38] *Frankfurt Institute for Advanced Studies, Johann Wolfgang Goethe-Universität Frankfurt, Frankfurt, Germany*
[39] *Fudan University, Shanghai, China*
[40] *Gangneung-Wonju National University, Gangneung, Republic of Korea*
[41] *Gauhati University, Department of Physics, Guwahati, India*
[42] *Helmholtz-Institut für Strahlen- und Kernphysik, Rheinische Friedrich-Wilhelms-Universität Bonn, Bonn, Germany*
[43] *Helsinki Institute of Physics (HIP), Helsinki, Finland*
[44] *High Energy Physics Group, Universidad Autónoma de Puebla, Puebla, Mexico*
[45] *Horia Hulubei National Institute of Physics and Nuclear Engineering, Bucharest, Romania*
[46] *HUN-REN Wigner Research Centre for Physics, Budapest, Hungary*
[47] *Indian Institute of Technology Bombay (IIT), Mumbai, India*
[48] *Indian Institute of Technology Indore, Indore, India*
[49] *INFN, Laboratori Nazionali di Frascati, Frascati, Italy*
[50] *INFN, Sezione di Bari, Bari, Italy*
[51] *INFN, Sezione di Bologna, Bologna, Italy*
[52] *INFN, Sezione di Cagliari, Cagliari, Italy*
[53] *INFN, Sezione di Catania, Catania, Italy*
[54] *INFN, Sezione di Padova, Padova, Italy*
[55] *INFN, Sezione di Pavia, Pavia, Italy*
[56] *INFN, Sezione di Torino, Turin, Italy*
[57] *INFN, Sezione di Trieste, Trieste, Italy*
[58] *Inha University, Incheon, Republic of Korea*
[59] *Institute for Gravitational and Subatomic Physics (GRASP), Utrecht University/Nikhef, Utrecht, The Netherlands*
[60] *Institute of Experimental Physics, Slovak Academy of Sciences, Košice, Slovak Republic*
[61] *Institute of Physics, Homi Bhabha National Institute, Bhubaneswar, India*
[62] *Institute of Physics of the Czech Academy of Sciences, Prague, Czech Republic*
[63] *Institute of Space Science (ISS), Bucharest, Romania*
[64] *Institut für Kernphysik, Johann Wolfgang Goethe-Universität Frankfurt, Frankfurt, Germany*
[65] *Instituto de Ciencias Nucleares, Universidad Nacional Autónoma de México, Mexico City, Mexico*
[66] *Instituto de Física, Universidade Federal do Rio Grande do Sul (UFRGS), Porto Alegre, Brazil*
[67] *Instituto de Física, Universidad Nacional Autónoma de México, Mexico City, Mexico*
[68] *iThemba LABS, National Research Foundation, Somerset West, South Africa*
[69] *Jeonbuk National University, Jeonju, Republic of Korea*
[70] *Johann-Wolfgang-Goethe Universität Frankfurt Institut für Informatik, Fachbereich Informatik und Mathematik, Frankfurt, Germany*
[71] *Korea Institute of Science and Technology Information, Daejeon, Republic of Korea*
[72] *KTO Karatay University, Konya, Turkey*
[73] *Laboratoire de Physique Subatomique et de Cosmologie, Université Grenoble-Alpes, CNRS-IN2P3, Grenoble, France*

JHEP08(2024)234

[74] Lawrence Berkeley National Laboratory, Berkeley, California, United States
[75] Lund University Department of Physics, Division of Particle Physics, Lund, Sweden
[76] Nagasaki Institute of Applied Science, Nagasaki, Japan
[77] Nara Women's University (NWU), Nara, Japan
[78] National and Kapodistrian University of Athens, School of Science, Department of Physics, Athens, Greece
[79] National Centre for Nuclear Research, Warsaw, Poland
[80] National Institute of Science Education and Research, Homi Bhabha National Institute, Jatni, India
[81] National Nuclear Research Center, Baku, Azerbaijan
[82] National Research and Innovation Agency - BRIN, Jakarta, Indonesia
[83] Niels Bohr Institute, University of Copenhagen, Copenhagen, Denmark
[84] Nikhef, National institute for subatomic physics, Amsterdam, The Netherlands
[85] Nuclear Physics Group, STFC Daresbury Laboratory, Daresbury, United Kingdom
[86] Nuclear Physics Institute of the Czech Academy of Sciences, Husinec-Řež, Czech Republic
[87] Oak Ridge National Laboratory, Oak Ridge, Tennessee, United States
[88] Ohio State University, Columbus, Ohio, United States
[89] Physics department, Faculty of science, University of Zagreb, Zagreb, Croatia
[90] Physics Department, Panjab University, Chandigarh, India
[91] Physics Department, University of Jammu, Jammu, India
[92] Physics Program and International Institute for Sustainability with Knotted Chiral Meta Matter (SKCM2), Hiroshima University, Hiroshima, Japan
[93] Physikalisches Institut, Eberhard-Karls-Universität Tübingen, Tübingen, Germany
[94] Physikalisches Institut, Ruprecht-Karls-Universität Heidelberg, Heidelberg, Germany
[95] Physik Department, Technische Universität München, Munich, Germany
[96] Politecnico di Bari and Sezione INFN, Bari, Italy
[97] Research Division and ExtreMe Matter Institute EMMI, GSI Helmholtzzentrum für Schwerionenforschung GmbH, Darmstadt, Germany
[98] Saga University, Saga, Japan
[99] Saha Institute of Nuclear Physics, Homi Bhabha National Institute, Kolkata, India
[100] School of Physics and Astronomy, University of Birmingham, Birmingham, United Kingdom
[101] Sección Física, Departamento de Ciencias, Pontificia Universidad Católica del Perú, Lima, Peru
[102] Stefan Meyer Institut für Subatomare Physik (SMI), Vienna, Austria
[103] SUBATECH, IMT Atlantique, Nantes Université, CNRS-IN2P3, Nantes, France
[104] Sungkyunkwan University, Suwon City, Republic of Korea
[105] Suranaree University of Technology, Nakhon Ratchasima, Thailand
[106] Technical University of Košice, Košice, Slovak Republic
[107] The Henryk Niewodniczanski Institute of Nuclear Physics, Polish Academy of Sciences, Cracow, Poland
[108] The University of Texas at Austin, Austin, Texas, United States
[109] Universidad Autónoma de Sinaloa, Culiacán, Mexico
[110] Universidade de São Paulo (USP), São Paulo, Brazil
[111] Universidade Estadual de Campinas (UNICAMP), Campinas, Brazil
[112] Universidade Federal do ABC, Santo Andre, Brazil
[113] Universitatea Nationala de Stiinta si Tehnologie Politehnica Bucuresti, Bucharest, Romania
[114] University of Cape Town, Cape Town, South Africa
[115] University of Houston, Houston, Texas, United States
[116] University of Jyväskylä, Jyväskylä, Finland
[117] University of Kansas, Lawrence, Kansas, United States
[118] University of Liverpool, Liverpool, United Kingdom
[119] University of Science and Technology of China, Hefei, China
[120] University of South-Eastern Norway, Kongsberg, Norway
[121] University of Tennessee, Knoxville, Tennessee, United States
[122] University of the Witwatersrand, Johannesburg, South Africa
[123] University of Tokyo, Tokyo, Japan
[124] University of Tsukuba, Tsukuba, Japan

JHEP08(2024)234

[125] Universität Münster, Institut für Kernphysik, Münster, Germany
[126] Université Clermont Auvergne, CNRS/IN2P3, LPC, Clermont-Ferrand, France
[127] Université de Lyon, CNRS/IN2P3, Institut de Physique des 2 Infinis de Lyon, Lyon, France
[128] Université de Strasbourg, CNRS, IPHC UMR 7178, F-67000 Strasbourg, France
[129] Université Paris-Saclay, Centre d'Etudes de Saclay (CEA), IRFU, Département de Physique Nucléaire (DPhN), Saclay, France
[130] Université Paris-Saclay, CNRS/IN2P3, IJCLab, Orsay, France
[131] Università degli Studi di Foggia, Foggia, Italy
[132] Università del Piemonte Orientale, Vercelli, Italy
[133] Università di Brescia, Brescia, Italy
[134] Variable Energy Cyclotron Centre, Homi Bhabha National Institute, Kolkata, India
[135] Warsaw University of Technology, Warsaw, Poland
[136] Wayne State University, Detroit, Michigan, United States
[137] Yale University, New Haven, Connecticut, United States
[138] Yonsei University, Seoul, Republic of Korea
[139] Zentrum für Technologie und Transfer (ZTT), Worms, Germany
[140] Affiliated with an institute covered by a cooperation agreement with CERN
[141] Affiliated with an international laboratory covered by a cooperation agreement with CERN.

[I] Deceased
[II] Also at: Max-Planck-Institut fur Physik, Munich, Germany
[III] Also at: Italian National Agency for New Technologies, Energy and Sustainable Economic Development (ENEA), Bologna, Italy
[IV] Also at: Dipartimento DET del Politecnico di Torino, Turin, Italy
[V] Also at: Yildiz Technical University, Istanbul, Türkiye
[VI] Also at: Department of Applied Physics, Aligarh Muslim University, Aligarh, India
[VII] Also at: Institute of Theoretical Physics, University of Wroclaw, Poland
[VIII] Also at: An institution covered by a cooperation agreement with CERN

JHEP08(2024)234